Biogeosciences
Discussions

Twenty-first century ocean warming, acidification, deoxygenation, and upper ocean nutrient decline from CMIP6 model projections

Lester Kwiatkowski[1], Olivier Torres[2], Laurent Bopp[2], Olivier Aumont[1], Matthew Chamberlain[3], James Christian[4], John P. Dunne[5], Marion Gehlen[6], Tatiana Ilyina[7], Jasmin G. John[5], Andrew Lenton[3], Hongmei Li[7], Nicole S. Lovenduski[8], James C. Orr[6], Julien Palmieri[9], Jörg Schwinger[10], Roland Séférian[11], Charles A. Stock[5], Alessandro Tagliabue[12], Yohei Takano[7], Jerry Tjiputra[10], Katsuya Toyama[13], Hiroyuki Tsujino[13], Michio Watanabe[14], Akitomo Yamamoto[14], Andrew Yool[9], Tilo Ziehn[3]

[1]LOCEAN Laboratory, Sorbonne Université-CNRS-IRD-MNHN, Paris, 75005, France
[2]LMD-IPSL, CNRS, Ecole Normale Supérieure / PSL Res. Univ, Ecole Polytechnique, Sorbonne Université, Paris, 75005, France
[3]CSIRO Oceans and Atmosphere, Hobart, TAS 7000, Australia
[4]Canadian Centre for Climate Modelling and Analysis, Victoria, BC, Canada
[5]NOAA Geophysical Fluid Dynamics Laboratory Princeton, New Jersey, USA
[6]Laboratoire des Sciences du Climat et de l'Environnement, LSCE-IPSL, CEA-CNRS-UVSQ, Université Paris Saclay, Gif-sur-Yvette, France
[7]Max Planck Institute for Meteorology, Bundesstraße 53, 20146 Hamburg, Germany
[8]Department of Atmospheric and Oceanic Sciences and Institute of Arctic and Alpine Research, University of Colorado, Boulder, Colorado, USA
[9]National Oceanography Centre, European Way, Southampton, SO14 3ZH, UK
[10]NORCE Climate, Bjerknes Centre for Climate Research, Bergen, Norway
[11]CNRM, Université de Toulouse, Météo-France, CNRS, Toulouse, France
[12]School of Environmental Sciences, University of Liverpool, United Kingdom
[13]Meteorological Research Institute, Japan Meteorological Agency, Tsukuba, Japan
[14]Research Center for Environmental Modeling and Application, Japan Agency for Marine-Earth Science and Technology (JAMSTEC), Yokohama, Japan

Correspondence to: Lester Kwiatkowski (lester.morgan-kwiatkowski@locean-ipsl.upmc.fr)

Abstract. Anthropogenic climate change leads to ocean warming, acidification, deoxygenation and reductions in near-surface nutrient concentrations, all of which are expected to affect marine ecosystems. Here we assess projections of these drivers of environmental change over the twenty-first century from Earth system models (ESMs) participating in the Coupled Model Intercomparison Project Phase 6 (CMIP6) that were forced under the CMIP6 Shared Socioeconomic Pathways (SSPs). Projections are compared to those from the previous generation (CMIP5) forced under the Representative Concentration Pathways (RCPs). 10 CMIP5 and 13 CMIP6 models are used in the two multi-model ensembles. Under the high-emission scenario SSP5-8.5, the model mean change (2080-2099 mean values relative to 1870-1899) in sea surface temperature, surface pH, subsurface (100-600 m) oxygen concentration and euphotic (0-100 m) nitrate concentration is $+3.48\pm0.78$ °C, -0.44 ± 0.005, -13.27 ± 5.28 mmol m^{-3} and -1.07 ± 0.45 mmol m^{-3}, respectively. Under the low-emission, high-mitigation scenario SSP1-2.6, the corresponding changes are $+1.42\pm0.32$ °C, -0.16 ± 0.002, -6.36 ± 2.92 mmol m^{-3} and -0.53 ± 0.23 mmol m^{-3}. Projected exposure of the marine ecosystem to these drivers of ocean change depends largely on the extent of future emissions, consistent with previous studies. The Earth system models in CMIP6 generally project greater surface warming, acidification, deoxygenation and euphotic nitrate reductions than those from CMIP5 under comparable radiative forcing, with no reduction in inter-model uncertainties. Under the high-emission CMIP5 scenario RCP8.5, the corresponding changes in sea surface temperature, surface pH, subsurface oxygen and euphotic nitrate concentration are $+3.04\pm0.62$ °C, -0.38 ± 0.005, -9.51 ± 2.13 mmol m^{-3} and -0.66 ± 0.49

Biogeosciences
Discussions

mmol m^{-3}, respectively. The greater surface acidification in CMIP6 is primarily a consequence of the SSPs
50 having higher associated atmospheric CO_2 concentrations than their RCP analogues. The increased projected
warming results from a general increase in the climate sensitivity of CMIP6 models relative to those of CMIP5.
This enhanced warming results in greater increases in upper ocean stratification in CMIP6 projections, which
contributes to greater reductions in euphotic nitrate and subsurface oxygen ventilation.

55 **1.   Introduction**

1.1   Ocean warming, acidification, deoxygenation and enhanced nutrient limitation

Since the preindustrial period the global oceans have experienced fundamental change in physical and
geochemical conditions as a result of anthropogenic climate change. Although these physicochemical changes
60 reflect the climate services that the oceans provide through heat and carbon storage, they also have major
implications for the health of marine ecosystems.

Temperature is a principal determinant of biological metabolism in the ocean (e.g. Eppley, 1972) and plays a
major role in shaping the global distribution of marine species (e.g. Thomas et al., 2012; Sunagawa et al., 2015).
65 The radiative forcing associated with greenhouse gas emissions results in an accumulation of heat in the Earth
system, most of which is taken up by the oceans (Frölicher et al., 2014). Global sea surface temperature (SST)
has increased by +0.7 °C over the last 100 years (Bindoff et al., 2007), with observations indicating that the rate
of warming in the upper 2000 m of the ocean has increased from 0.55 to 0.68 W m^{-2} since 1991 (Cheng et al.,
2019).

70

Earth system models project 21st century increases in SST under all of the RCPs (Bopp et al., 2013). While
certain species may have the potential to acclimate to rising ocean temperatures, poleward range shifts of many
species have already been observed (Gregory et al., 2009; Sorte et al., 2010), with associated declines in tropical
diversity projected (Thomas et al., 2012). Concurrently, the frequency, intensity and duration of ocean heat
75 waves has increased in the observational record and is projected to substantially increase in the future (Frölicher
et al., 2018). This has already had serious impacts on marine foundation taxa such as corals, seagrasses and kelps
(Garrabou et al., 2009; Hobday et al., 2016; Smale et al., 2019).

A consequence of ocean warming is an increase in vertical density gradients and enhanced stratification. This
80 results in a reduction in the supply of nutrients to the euphotic zone, with enhanced nutrient limitation generally
leading to observed declines in net primary production (Behrenfeld et al., 2001; Behrenfeld et al., 2006). Earth
system model projections consistently show enhanced stratification and associated reductions in euphotic
nutrient concentrations under scenarios of climate change (Bopp et al., 2001; Sarmiento et al., 2004; Cabré et al.,
2014; Fu et al., 2016). This generally results in projected global reductions in primary production that are driven
85 by enhanced phytoplankton nutrient limitation in the low-latitude oceans (Steinacher et al., 2010; Bopp et al.,
2013; Krumhardt et al. 2017; Kwiatkowski et al., 2017; Moore et al., 2018). The projected magnitude of primary
production declines is highly uncertain across model ensembles (Bopp et al., 2013; Krumhardt et al. 2017), in
part due to concurrent changes in phytoplankton light and temperature limitation, as well as altered top-down

90   grazing, all of which can compensate for nutrient-driven production declines (Taucher and Oschlies, 2011; Laufkötter et al., 2015). However, declines in phytoplankton primary production are consistently amplified in higher trophic levels such as zooplankton (Chust et al., 2014; Stock et al., 2014; Kwiatkowski et al., 2018) and fish (Lotze et al., 2019).

95   Dissolved oxygen in the ocean exerts a strong control on marine ecosystems. At low O_2 levels, marine animals are unable to sustain aerobic metabolism, which can lead to mortality (Vaquer-Sunyer and Duarte, 2008). Oxygen levels also affect many oceanic biogeochemical cycles through an impact on redox reactions and microbial metabolism (e.g. on the nitrogen cycle, Gruber, 2004).

100   Global warming is driving a global decline of dissolved oxygen in the ocean, referred to as ocean deoxygenation, because of a warming-induced reduction in O_2 solubility and increased stratification / reduced ventilation (Keeling et al., 2010; Oschlies et al., 2018). A recent assessment, based on three different analyses (Helm et al., 2011; Schmidtko et al., 2017; Ito et al., 2017) concluded that the oxygen content over the first 1000 m of the ocean has decreased by 0.5 to 3.3 % over 1970-2010 (Bindoff, et al., in press). In coastal systems, this warming effect is exacerbated by the effects of increased loading of nutrients and organic matter, which also lead to

105   oxygen decline and an increase in coastal ocean dead zones (Breitburg et al., 2018). Earth System model projections consistently show continuing declines in oxygen over the 21st century as a function of the employed scenario (Bopp et al., 2013; Cocco et al., 2013), with large uncertainties in the tropics and for the evolution of oxygen minimum zones (Cabré et al., 2015).

110   The uptake of carbon by the oceans affects marine chemistry via ocean acidification (Gattuso and Buddemeier, 2000; Orr et al., 2005; Doney et al., 2009), a process that increases seawater concentrations of CO_2, H^+ and HCO_3^-, and reduces levels of pH and CO_3^{2-}. The oceans have absorbed approximately 30% of anthropogenic carbon emissions since the pre-industrial (Sabine et al., 2004; Khatiwala et al., 2009; Khatiwala et al., 2013; Gruber et al., 2019), resulting in global surface pH declines of approximately 0.1 units (Bindoff et al., 2007).

115   Declines in open ocean surface pH are 0.018 per decade over 1991-2011 (Lauvset et al. 2015), while Earth system models have projected 21st century global surface ocean pH declines of up to 0.33 units under previous high emissions scenarios (Bopp et al., 2013), with associated changes in the seasonal cycles of seawater carbonate chemistry (McNeil and Sasse, 2016; Kwiatkowski and Orr, 2018; Landschützer et al., 2018).

120   The impact of ocean acidification on marine species is extensive and diverse. Calcifying species, such as echinoderms, bryozoans and cnidarians, exhibit depressed calcification, growth and survival under acidification (Kroeker et al., 2010; Albright et al., 2016; Kwiatkowski et al., 2016), altering the competitive balance in ecosystems (Kroeker et al., 2013). In teleost fish and marine invertebrates, ion exchange is reduced under acidification, depressing protein synthesis and metabolic rates (Langenbuch et al., 2006; Pörtner, 2008).

125   Physiological and behavioural functioning is also sensitive to acidification, with olfactory discrimination (Munday et al., 2009) and predator-prey responses (Watson et al., 2014; Watson et al., 2017) shown to be impaired under more acidified conditions.

130   Marine organisms typically experience changes in multiple physical and geochemical conditions simultaneously, with impacts determined by the interactions between potential stressors. For example, the combined effect of warming and deoxygenation is projected to force poleward and vertical contractions of metabolically viable habitat for marine ectotherms (Deutsch et al., 2015). At the physiological level, experimental studies indicate that synergistic effects between potential marine stressors are common (Gunderson et al., 2016). Compound

135   warming and acidification, has been shown to exacerbate negative impacts on photosynthesis, calcification, reproduction and survival of marine organisms (Harvey et al., 2013), while compound exposure to acidification and low oxygen can also have synergistic effects (McBryan et al., 2013), and may reduce the thermal tolerance of certain species (Pörtner, 2010).

140   Here we assess future projections of climate-related drivers of marine impacts within the Coupled Model Intercomparison Project Phase 6 (CMIP6; Eyring et al., 2016; O'Neill et al., 2016) simulations, evaluating how these differ from previous CMIP5 (Taylor et al., 2011) simulations. We focus on projected changes in ocean temperature, pH and dissolved O_2 and NO_3^- concentration across 13 CMIP6 and 10 CMIP5 Earth system models.

1.2   Ocean biogeochemical model development since CMIP5

145

A comprehensive assessment of changes between CMIP5 and CMIP6 in the ocean biogeochemical components of ESMs and their associated skill is provided in Séférian et al, (in review). Since CMIP5, CMIP6 has seen a general increase in the horizontal grid resolution of physical ocean models and a limited increase in vertical resolution. The latter may be particularly important for ecosystem projections as it directly affects simulated

150   stratification, a key factor influencing changes in ocean impact drivers (Capotondi et al., 2012; Bopp et al., 2013; Laufkötter et al., 2015; Kwiatkowski et al., 2017) and their impact on higher trophic levels (Stock et al., 2014; Chust et al., 2014; Kwiatkowski et al., 2018; Lotze et al., 2019). Updates in the representation of ocean biogeochemical processes between CMIP5 and CMIP6 have generally included increases in model complexity (Séférian et al., in review). Specifically, CMIP6 models provide more widespread inclusion of micronutrients,

155   such as iron, variable stoichiometric ratios, and improved representation of lower trophic levels including bacteria and the cycling and sinking of organic matter (Séférian et al., in review).

Relative to CMIP5, the skill of the CMIP6 Earth system models is improved in terms of their skill in simulating the mean state of selected biogeochemical tracers (Séférian et al, in review). The global representation of

160   present-day mean state air-sea CO_2 fluxes and surface chlorophyll concentrations show moderate improvements between CMIP5 and CMIP6. There are also moderate improvements in the representation of subsurface dissolved oxygen concentrations in most ocean basins. Model skill in the representation of surface macronutrient concentrations in CMIP6 has improved for total dissolved silicon but declined slightly for nitrate.

165   ## 2.   Methodology

The analysis of projected multiple ocean impact drivers presented here focuses on three key depth levels: the upper ocean, the thermocline, and the benthic zone. The surface zone is where most biological activity is

170 concentrated in the oceans and where impacts from climate change are typically greatest. Specifically, we assess projections of surface ocean temperature, surface ocean pH, subsurface dissolved O_2 concentration (averaged between 100-600 m) and upper-ocean NO_3^- concentration (averaged between 0-100 m). The choice of vertical integral for O_2 reflects the potential importance of the expansion of oxygen minimum zones, which are most prominent at such depths. The choice of vertical integral for NO_3^- reflects its importance as a critical macronutrient supporting primary production in the euphotic zone. Both vertical integrals are chosen to be

175 compatible with the recent assessment of marine drivers in the IPCC Special Report on the Ocean and Cryosphere (Bindoff, et al., in press). Additionally, for the CMIP6 models we assess benthic ecosystem drivers, focussing on projections of bottom temperature, pH and O_2 concentration. The benthic level is defined as the bottom ocean model layer at each grid point. As such, its exact depth depends on vertical discretisation and bathymetry, which differs across the CMIP6 ensemble. All benthic model outputs were corrected for potential

180 drift (e.g. Gehlen et al., 2014; Séférian et al., 2016) using coincident preindustrial control simulations.

2.1   Processing and analysis of model outputs

All ESMs assessed in the CMIP5 and CMIP6 ensembles (Tables 1 and 2) include physical ocean models and

185 coupled ocean biogeochemistry schemes that account for some or all of the potential ocean impact drivers: temperature, pH, O_2 and NO_3^- concentration. A total of 10 CMIP5 and 13 CMIP6 models are assessed with the model ensemble size differing among scenarios depending on contributions from each model group. The CMIP5 ensemble is the same as that used in the comprehensive assessment of projected ocean drivers provided by Bopp et al. (2013). Only one ensemble member per model is used for a given scenario. That is, in CMIP terminology

190 we typically use ensemble member 'r1i1p1' from each CMIP5 model and 'r1i1p1fx' from each CMIP6 model (where 'fx' is the best available set of external forcings employed by the various modelling groups) Consequently, we do not assess the role of internal variability in the emergence of climate-related changes in marine ecosystems drivers (e.g. Frölicher et al., 2016; Lovenduski et al., 2016; Krumhardt et al. 2017; Freeman et al., 2018). Two of the CMIP6 models included in our analysis (GFDL-CM4 and ACCESS-ESM1.5) do not

195 include NO_3^- as a prognostic tracer. Hence their NO_3^- concentrations were calculated from modelled total dissolved inorganic phosphorus assuming a constant Redfield ratio of 16:1.

To facilitate intercomparison, model output on each native grid was regridded to the same regular 1°x1° horizontal grid using distance weighted average remapping (climate data operators; remapdis). Model outputs

200 were kept on their native vertical grids, with vertical discretisation ranging from 40 (MPI-ESM1.2) to 75 (IPSL-CM6A-LR, CNRM-ESM2-1 and UKESM1-0-LL) levels, except for models using hybrid or isopycnic vertical coordinates (GFDL-ESM4, GFDL-CM4, NorESM2-LM) for which model outputs were vertically regridded. Following generally adopted practice (e.g. Bopp et al., 2013), all models were given equal weighting in the respective CMIP6 and CMIP5 ensemble mean. However, within the CMIP6 ensemble two modelling groups

205 contributed two ESMs and within the CMIP5 ensemble three modelling groups contributed two ESMs, which is likely to influence the extent of model independence (Masson and Knutti, 2011; Knutti et al., 2015; Sanderson et al., 2015; Lovenduski et al. 2017).

210 The CMIP5 historical simulations had variable start dates between 1850 and 1861, all of which finished in 2005; the subsequent RCP simulations started in 2006 and were run until at least 2099. In CMIP6, there is greater temporal consistency. All CMIP6 historical simulations were made over 1850-2014, while the subsequent SSP scenarios started in 2015 and ran until at least 2100. To facilitate comparison between CMIP5 and CMIP6, the historical and future projections of ocean impact drivers in both phases of CMIP are presented as anomalies relative to 1870-1899 mean values of their respective historical simulations. When solely evaluating 21st century

215 projections in the SSPs however, the last 20 years of the CMIP6 historical simulations (1995-2014) are used as a baseline period.

2.2 From Representative Concentration Pathways to Shared Socioeconomic Pathways

220 Aside from changes in ESMs, a fundamental difference between CMIP5 and CMIP6 is that they differ in the future scenarios used for anthropogenic emissions and land-use change. Those scenarios are derived from integrated assessment models and based on plausible future pathways of societal development. In CMIP6, the Shared Socioeconomic Pathways (SSPs) provided via the Scenario Model Intercomparison Project (ScenarioMIP) are used instead of the Representative Concentration Pathways (RCPs) that were used in CMIP5

225 (O'Neill et al., 2016). The SSPs provide revised emission and land-use scenarios relative to the RCPs (Riahi et al., 2017).

In this study, we confine our assessment of ocean impact drivers to concentration-driven simulations, focussing on SSP1-2.6, SSP2-4.5, SSP3-7.0 and SSP5-8.5 of CMIP6, which result in end-of-century radiative forcing of

230 2.6, 4.5, 7.0 and 8.5 W m^{-2}, respectively. The SSPs have generally higher associated concentrations of atmospheric CO_2 and lower associated atmospheric concentrations of CH_4 and N_2O relative to their RCP counterparts (Meinshausen et al., 2011; O'Neill et al., 2016; Meinshausen et al., 2019). This is particularly the case for SSP5-8.5, which in comparison to RCP8.5, assumes that coal constitutes a greater proportion of the primary energy mix in the second half of the 21st century (Kriegler et al., 2017). Given that differences among

235 projections of surface ocean acidification are dominated by scenario uncertainty, with relatively little model structural uncertainty and internal variability (e.g. Bopp et al., 2013; Frölicher et al., 2016), such changes in atmospheric concentrations of CO_2 are expected to have a large impact on projections of ocean pH and related carbonate system variables.

240 Alongside the assessment of the SSP-forced model outputs, outputs from models forced under the four RCPs (RCP2.6, RCP4.5, RCP6.0 and RCP8.5) are also assessed in parallel. This allows some comparison with past CMIP5 assessments (e.g. Bopp et al., 2013). However, RCP6.0 has no direct SSP analogue, while SSP3-7.0 has no direct RCP analogue.

245 ## 3. Results and discussion

3.1 Global upper-ocean projections

250 Under all SSPs, sea surface temperature is projected to increase, while surface pH, subsurface dissolved oxygen concentrations and euphotic-zone nitrate concentrations are projected to decline during the twenty-first century (Fig. 1). The projected change in the four ocean impact drivers increases with associated radiative forcing across the four SSPs. Under the high mitigation SSP1-2.6 scenario, the end-of-century model mean changes (2080-2099 mean values relative to 1870-1899) in sea surface temperature, surface pH, subsurface oxygen concentration and euphotic nitrate concentration are +1.42±0.32 °C, -0.16±0.002, -6.36±2.92 mmol m^{-3} and -

255 0.53±0.23 mmol m^{-3}, respectively. Under the high emissions scenario SSP5-8.5 the corresponding changes are 3.48±0.78 °C, -0.44±0.005, -13.27±5.28 mmol m^{-3} and -1.07±0.45 mmol m^{-3} (Table 3), respectively. As the changes have no statistical overlap across the two scenarios (with the exception of subsurface oxygen), the CMIP6 projections further demonstrate the effectiveness of intense mitigation strategies in limiting twenty-first century marine ecosystem exposure to potential stress. This is in agreement with assessments of previous multi-

260 model projections (e.g. CMIP5; Bopp et al., 2013).

Following previous assessments (Bopp et al., 2013), model structural uncertainty is estimated as the inter-model standard deviation. Although some of this model spread is due to internal variability, this contribution is relatively small for global averages and expected to decline throughout the twenty-first century (Frölicher et al.,

265 2016). Relative to scenario uncertainty, which is estimated as the maximum difference between mean SSP projections, model structural uncertainty is extremely low for surface pH projections, which show distinct separation between the SSPs prior to 2050. The low model structural uncertainty associated with projections of surface ocean pH is well characterised and associated with the identical CO_2 forcing used by all ESMs in concentration-driven SSP and RCP projections (Lovenduski et al., 2016), a weak climate-pH feedback (Orr et

270 al., 2005; McNeil and Matear, 2007), limited interannual variability and consistently adopted standards for ESM ocean carbonate chemistry equations (Orr et al., 2017). Surface ocean pCO$_2$ and corresponding carbonate chemistry generally follows changes in atmospheric CO_2 with a global mean equilibration time of approximately 8 months (Gattuso and Hansson, 2011). The differences between projected surface pH across the SSPs therefore reflect the divergence of prescribed atmospheric CO_2 concentrations, i.e., the different scenarios.

275

In contrast, projections of SST exhibit greater model structural uncertainty (Fig. 1). This uncertainty is likely to result from differences in climate sensitivity between models. Historically, such differences have been attributed to diversity in cloud feedbacks and to a lesser extent water vapour and lapse-rate feedbacks (Andrews et al., 2012; Vial et al., 2013). For projections of subsurface oxygen and euphotic-zone nitrate concentrations, model

280 structural uncertainty is greater still and can exceed scenario uncertainty. This greater structural uncertainty is a result of oxygen and nitrate concentrations being strongly influenced by both physical changes (e.g. changes in solubility, circulation and mixing) and changes in biological sources and sinks (Stramma et al., 2012; Fu et al., 2016; Bopp et al., 2017; Oschlies et al., 2018).

285 **3.2 Regional patterns of upper-ocean change**

Global scale projections of end-of-century upper-ocean impact drivers (2080-2099 anomalies relative to 1995-2014 mean values) exhibit spatial variability that is both ocean impact driver and SSP dependent (Fig. 2).

290   CMIP6 projections of SST show near global relatively uniform increases under both SSP1-2.6 and SSP5-8.5, with the greatest warming evident in the Northern Hemisphere, particularly the Arctic Ocean and high-latitude North Pacific, where mean model warming can exceed 2°C in SSP1-2.6 and 5°C in SSP5-8.5. This Arctic amplification is well established in both observations (Bekryaev et al., 2010) and models, and thought to be primarily driven by temperature and surface albedo feedbacks (Screen and Simmonds, 2010; Pithan and Mauritsen, 2014). The notable exception to warming is in the subpolar North Atlantic where there is minor

295   cooling in SSP1-2.6 and limited warming in SSP5-8.5. This 'warming hole' is also well documented in both observations and models and typically related to a slow down in the Atlantic meridional overturning circulation (Drijfhout et al., 2012; Menary and Wood, 2018). Spatial patterns of SST anomalies are broadly consistent with those of the CMIP5 ensemble (Bopp et al., 2013).

300   Anomalies in surface ocean pH are ubiquitously negative under both SSP1-2.6 and SSP5-8.5, with very low associated model structural uncertainty. Consistent with past model projections (McNeil and Matear, 2007; Steinacher et al., 2009; Bopp et al., 2013), the greatest declines in pH are projected in the higher latitudes and especially the Arctic Ocean, where model mean declines can exceed 0.45 in SSP5-8.5 (2080-2099 anomalies relative to 1995-2014; Fig. 2c,d). This enhanced Arctic Ocean acidification reflects the role of sea ice loss in

305   enhancing anthropogenic carbon uptake through gas exchange and the effects of dilution with freshwater from ice melt (McNeil and Matear, 2007; Steinacher et al., 2009; Yamamoto-Kawai et al., 2009; Yamamoto et al., 2012).

        Although global mean subsurface (100-600 m) O_2 concentration is projected to decline under all SSPs, there is a

310   high degree of variability in projections at regional scales (Fig. 2e,f). The largest declines in subsurface O_2 generally occur at higher latitudes and in particular in the North Pacific, where declines in the model mean can exceed 40 mmol m^{-3} in SSP5-8.5. In equatorial regions of the Atlantic and Indian Ocean and upwelling regions of the Pacific, increases in subsurface O_2 concentration are projected under both SSP1-2.6 and SSP5-8.5. These increases are at odds with historical observations of expanding OMZs (Stramma et al., 2008), which may be a

315   result of climate variability (Deutsch et al., 2011; Bindoff et al., in press). They are however, in line with previous projections, including those from CMIP5, which have highlighted that coarse-resolution models struggle to reproduce subsurface ventilation pathways in these regions (Stramma et al., 2012; Andrews et al., 2013; Bopp et al., 2013; Cabré et al., 2015).

320   For a subset of the CMIP6 models, projected changes in subsurface O_2 concentration under SSP5-8.5 were decomposed into changes in O_2 saturation (O_{2sat}) and apparent oxygen utilisation (AOU), where $\Delta O_2 = \Delta O_{2sat} - \Delta AOU$ (Fig. 3). O_{2sat} was computed from model temperature and salinity outputs and represents the effect of oxygen solubility changes on dissolved O_2 concentration, while AOU was calculated as $\Delta AOU = \Delta O_{2sat} - \Delta O_2$, and is affected by both changes in biological consumption of O_2 and in ventilation/stratification. The heightened

325   reductions in subsurface O_2 in the North Pacific and North Atlantic are shown to be the result of reductions in O_{2sat} and increases in AOU, which act to reinforce O_2 concentration declines. In contrast, the projected increases in O_2 in the tropical Indian and Atlantic Oceans are shown to be the result of reductions in AOU that more than compensate for concurrent reductions in O_{2sat}. The spatial patterns of CMIP6 projected changes in subsurface

O_{2sat} and AOU under SSP5-8.5 are similar to that of the CMIP5 models under RCP8.5 (Bopp et al., 2017). The
330 general reduction in O_{2sat} has been shown to be predominantly due to warming driven reductions in solubility,
while the heightened AOU declines in the North Pacific and North Atlantic have been attributed to reductions in
ventilation and an increase in the age of these waters (Bopp et al., 2017; Tjiputra et al., 2018).

CMIP6 model-mean projections of NO_3^- concentrations in the euphotic zone (0-100 m) show variable regional
335 declines under SSP1-2.6 and SSP5-8.5 (Fig. 2g,h). These declines are largest in the Arctic Ocean, equatorial
Eastern Pacific, North Atlantic and North Pacific where they can exceed 3 mmol m^{-3} in SSP5-8.5. NO_3^-
concentrations show limited anomalies in the subtropical gyres where concentrations are already very low. The
CMIP6 spatial pattern of euphotic-zone NO_3^- anomalies is in broad agreement with CMIP5 projections (Fu et al.,
2016), which show greater relative reductions in NO_3^- concentrations in regions of greater relative increase in
340 stratification.

The difference between densities at 200 m and the surface is used as an index of stratification in the CMIP6
projections. The global mean twenty-first century increase in stratification index is +0.15±0.04 kg m^{-3} and
+0.62±0.08 kg m^{-3} under SSP1-2.6 and SSP5-8.5, respectively (Fig. 4). Thus global mean stratification increases
345 with the radiative forcing associated with SSPs. For both SSP1-2.6 and SSP5-8.5, the greatest increases in
stratification index are projected in the Indian Ocean, the North Atlantic and the Equatorial and North Pacific,
where they can exceed +2 kg m^{-3} under SSP5-8.5. Increases in stratification in the Southern Ocean are limited.
This is partly due to the depth integral over which the index is defined but in the CMIP5 models was also
attributed to intensified surface westerlies (Swart and Fyfe, 2012), which increases surface-layer mixing and
350 upwelling in the Southern Ocean (Fu et al., 2016). Regions of enhanced stratification are typically projected to
experience reductions in euphotic NO_3^- concentrations, in agreement with previous projections (Bopp et al.,
2001; Cabré et al., 2014; Fu et al., 2016). An exception to this however, is in certain Arctic Seas, where there are
reductions in both stratification index and euphotic-zone NO_3^- concentrations. This is presumably a consequence
of the loss of permanent or semi-permanent sea ice and a corresponding increase in wind-driven mixing.

355

3.3   Potential exposure to compound stressors

The projected occurrence of multiple potential ecosystem stressors in the upper ocean was determined across the
SSPs using prescribed thresholds of surface warming (>+2 °C), surface acidification (< -0.2 units), subsurface
360 deoxygenation (< -30 mmol m^{-3}) and euphotic-zone NO_3^- decline (< -1 mmol m^{-3}; Fig. 5). The concurrent
exceedance of multiple thresholds increases with associated radiative forcing across the SSPs, indicative of
greater exposure to potential compound ecosystem stressors. The tropical and subtropical oceans are generally
characterised by projected exposure to compound warming and acidification under SSP3-7.0 and SSP5-8.5, with
additional nutrient thresholds exceeded in regions of equatorial upwelling. The North Pacific is characterised by
365 high sensitivity to potential compound stressors, with all thresholds of warming, acidification, deoxygenation
and nutrient decline exceeded under SSP5-8.5. In contrast, the projected occurrence of compound stressors is
limited in the Southern Ocean, where only the acidification threshold is consistently exceeded. The North

Atlantic is characterised by sensitivity to combined acidification and nutrient stress, while the Arctic Ocean is sensitive to compound warming, acidification and nutrient stress.

370

3.4   CMIP6 vs. CMIP5 projections

While the temporal behaviour of changes in ocean impact drivers is similar across the CMIP5 and CMIP6 model suites (Fig. 1), the CMIP6 Earth system models generally project greater global surface ocean warming, surface
375   ocean acidification, subsurface deoxygenation and euphotic-zone NO_3 reduction than the CMIP5 projections performed with comparable radiative forcing (Fig. 6, Table 3). There is no consistent reduction in model structural uncertainty between CMIP5 and CMIP6. The projected end-of-century SST increase (2080-2099 minus 1870-1899) in SSP1-2.6, SSP2-4.5 and SSP5-8.5 is +1.42±0.32 °C, +2.10± 0.43 °C and +3.48± 0.78 °C compared to +1.15±0.33 °C, +1.74±0.44 °C and +3.04±0.62 °C in RCP2.6, RCP4.5 and RCP8.5, respectively.
380   This enhanced CMIP6 warming is attributable to generally greater climate sensitivity in the CMIP6 model ensemble relative to the CMIP5 ensemble (Forster et al., 2019). Indeed, the MAGICC7.0 climate model projects marginally greater warming of near-surface air temperatures in the RCPs, than SSPs with the same end-of-century radiative forcing (Meinshausen et al., 2019).

385   The projected end-of-century pH decline in SSP1-2.6, SSP2-4.5 and SSP5-8.5 is -0.16±0.002, -0.26±0.003 and -0.44±0.005 compared to -0.14±0.001, -0.21±0.002 and -0.38±0.005 in RCP2.6, RCP4.5 and RCP8.5, respectively (Fig. 6, Table 3). Enhanced acidification in CMIP6 relative to CMIP5 is consistent across models and attributable to higher prescribed atmospheric CO_2 levels in the forcing of the SSP scenarios relative to the RCP scenarios with equivalent radiative forcing (Meinshausen et al., 2019). Year 2100 atmospheric CO_2 levels
390   are 1135.2 ppm, 602.8 ppm and 445.6 ppm in SSP5-8.5, SSP2-4.5 and SSP1-2.6, respectively. The corresponding levels in RCP8.5, RCP4.5 and RCP2.6 are 936 ppm, 538 ppm and 421 ppm (Meinshausen et al., 2011). Therefore although the SSP and RCP simulation pairs have analogous end-of-century radiative forcing, the higher CO_2 levels in the SSPs result in greater acidification for the CMIP6 projections.

395   The end-of-century euphotic-zone NO_3^- concentration decline in SSP1-2.6, SSP2-4.5 and SSP5-8.5 is -0.53±0.23, -0.66±0.32 and -1.07±0.45 mmol m^{-3} compared to -0.38±0.15, -0.51±0.14 and -0.66±0.49 mmol m^{-3} in RCP2.6, RCP4.5 and RCP8.5, respectively (Fig. 6, Table 3). The greater euphotic-zone NO_3^- concentration declines in SSPs compared to their RCP analogue is likely a consequence of the enhanced surface warming in CMIP6 models. This warming results in a greater increase in upper-ocean stratification than that projected in
400   CMIP5 models (Cabré et al., 2014; Fu et al., 2016), the result of which is a greater reduction in the supply of nutrient-rich deep waters to the euphotic zone in CMIP6 projections.

The end-of-century subsurface O_2 concentration decline in SSP1-2.6, SSP2-4.5 and SSP5-8.5 is -6.36 ±2.92, -8.14±4.08 and -13.27 ± 5.28 mmol m^{-3} compared to -3.71±2.47, -6.16±2.86 and -9.51±2.13 mmol m^{-3} in
405   RCP2.6, RCP4.5 and RCP8.5, respectively (Fig. 6, Table 3). The greater projected decline in subsurface O_2 concentration in the SSPs is the consequence of both physical and biogeochemical processes (e.g. Bopp et al., 2017; Oschlies et al., 2018). The enhanced warming in CMIP6 projections results in a greater reduction in O_2

solubility, while also affecting the ventilation and transport of O_2 within the ocean interior. In addition, concurrent changes in biological production, export and respiration can either mitigate or exacerbate physically

410   driven subsurface deoxygenation (Oschlies et al., 2018).

3.5   Global benthic ocean projections

On average, bottom waters are consistently projected to warm, acidify and deoxygenate across the twenty-first

415   century (Fig. 7). Under SSP1-2.6, the end-of-century model mean changes (2080-2099 relative to 1870-1899) in bottom-water temperature, pH and dissolved O_2 are +0.13±0.03 °C, -0.017±0.002 and -5.34±1.99 mmol m^{-3}, respectively. Under SSP5-8.5 the corresponding changes are +0.23±0.04 °C, -0.029±0.002 and -5.19±2.49 mmol m^{-3} (Table 4). Thus even for bottom waters, CMIP6 projections highlight that intense mitigation strategies can limit ecosystem exposure to potential warming and acidification stress during the twenty-first century (e.g.

420   Tittensor et al., 2010; Levin and Le Bris, 2015).

The magnitude of projected changes in bottom waters is less than in surface and upper-ocean waters, while bottom-water uncertainties for a given scenario are larger (Fig. 7). This contrast is particularly evident for pH projections with the SSPs, whose ranges of uncertainties fully separate before 2050 in the surface ocean (Fig. 1)

425   but still overlap in 2080 for bottom waters. This relative increase in model structural uncertainty results from surface ocean chemistry being in equilibrium with the same atmospheric CO_2 concentrations for all models. Conversely, benthic pH changes are strongly influenced by ocean circulation, which transports anthropogenic carbon in the upper ocean to the seafloor and is variably impacted by climate change across models (e.g. Gregory et al., 2005; Cheng et al., 2013). The increased uncertainty in pH projections with depth has been

430   previously noted for CMIP5 projections in the North Atlantic (Gehlen et al., 2014) and Arctic Ocean (Steiner et al., 2014). For projected global deoxygenation in bottom waters, model structural uncertainty is substantially larger than scenario uncertainty in CMIP6. As with projections of subsurface dissolved O_2, this larger model uncertainty results from the isolation of bottom waters from the atmosphere. Thus bottom waters at a given temperature and salinity may deviate substantially from the value that would be determined by their solubility

435   and air-sea equilibrium due to effects from other physical and biogeochemical processes (e.g. Oschlies et al., 2018).

3.6   Regional patterns of benthic ocean change

440   In bottom waters, the end-of-century spatial distributions of changes in temperature, pH and dissolved O_2 are similar between SSPs (Fig. 8) and in broad agreement with CMIP5 projections (Sweetman et al., 2017). The intensity of warming and acidification is typically greater in SSP5-8.5 than SSP1-2.6, particularly in coastal shelf regions and the Arctic Ocean. The largest projected benthic warming in SSP1-2.6 and SSP5-8.5 occurs in continental shelf waters, the Arctic Seas and the Southern Ocean, where temperature increases can exceed 0.6 °C

445   by the end-of-century (2080-2099 average relative to the 1995-2014 baseline). In contrast, for most of the abyssal benthic ocean projected increases in temperature are less than 0.2 °C. The characteristic North Atlantic "warming hole" present in projections of the surface ocean (Fig. 2) is also evident in benthic layers above 1000

m, such as the mid-Atlantic ridge. This represents the only region of consistent projected cooling across SSP1-2.6 and SSP5-8.5. As in the surface ocean, this cooling is likely associated with a slow down of the Atlantic

450   meridional overturning circulation (Drijfhout et al., 2012; Menary and Wood, 2018).

Projected end-of-century acidification is highly limited in most bottom waters, however in the North Atlantic, Arctic Seas and certain continental shelf waters, pH changes can exceed -0.1 in SSP1-2.6 and -0.3 in SSP5-8.5. For shelf waters, the greater bottom-water pH declines can be the result of coupling between surface waters,

455   which experience large changes in carbonate chemistry, and bottom waters (e.g. through mixing and entrainment), as well as benthic remineralization of organic matter (Bates et al., 2009). In contrast, enhanced bottom-water acidification in the North Atlantic is associated with deep-water formation and high uptake of anthropogenic carbon (Sabine et al., 2004), which rapidly propagates anomalies in surface ocean chemistry to depth. Bottom-water acidification has been previously projected in the North Atlantic by an ensemble of CMIP5

460   models under RCP8.5 (Gehlen et al., 2014; Sweetman et al., 2017).

In contrast to temperature and pH, projections of benthic dissolved O_2 concentration show changes that are not confined to shelf waters and specific regions. Most of the global benthic ocean is projected to experience deoxygenation under both SSP1-2.6 and SSP5-8.5, with only isolated coastal regions exhibiting benthic

465   oxygenation (Fig. 8). Bottom-water deoxygenation is highest in the North Atlantic and Southern Ocean where declines in the model mean can exceed 20 mmol m^{-3}. Although benthic deoxygenation is very similar under SSP1-2.6 and SSP5-8.5 in terms of the global mean (Fig. 7; Table 4), this is not always reflected regionally. The North Atlantic is projected to experience enhanced deoxygenation under SSP5-8.5 than SSP1-2.6, while in the equatorial Pacific and South Atlantic, greater deoxygenation is generally projected under SSP1-2.6.

470

3.7   Depth of maximum acidification

The depth of maximum end-of century pH and [H$^+$] change is often below the surface, and it varies regionally in CMIP6 projections (Fig. 9). Although the maximum pH change is usually found in surface waters in the high

475   latitudes and upwelling regions, it is typically located between 200-400 m in subtropical mode and intermediate waters. Because of its log scale, if the change in pH were identical in surface and subsurface waters it would imply a larger absolute change in [H$^+$] in the subsurface, where the mean [H$^+$] is higher. Indeed, a change in pH represents a relative change in [H$^+$], not an absolute change in that quantity. That relationship combined with higher [H$^+$] at depth, usually means that the maximum change in [H$^+$] is usually deeper than it is for pH.

480   Furthermore, the spatial distribution of the maximum change in pH and [H$^+$] also differ.

Enhanced acidification in subsurface mode and intermediate waters has been observed at time series stations (Dore et al., 2009; Byrne et al., 2010; Bates et al., 2012) and in CMIP5 model projections (Resplandy et al., 2013; Bopp et al., 2013; Watanabe and Kawamiya, 2017). Although observational studies have suggested that

485   this enhancement results from changes in circulation and biological activity (Dore et al., 2009; Byrne et al., 2010), model results indicate that it can be explained by the geochemical effect of rising atmospheric CO_2 and the particular carbonate chemistry of these waters (Orr, 2011; Resplandy et al., 2013). Specifically, the enhanced

490 acidification sensitivity in mode and intermediate waters has been attributed to their lower temperatures and their higher ratio of dissolved inorganic carbon to total alkalinity relative to that found in surface waters of the same regions (Orr, 2011; Resplandy et al., 2013).

3.8 Surface ocean seasonality

495 Changes in the seasonal amplitude of surface ocean temperature, pH and hydrogen concentration ([H^+]) were determined after detrending, by subtracting a cubic spline fit from the monthly time series in each grid cell, and then calculating the annual peak-to-peak amplitude for each year of the detrended data set, following the approach of Kwiatkowski and Orr (2018). Under SSP5-8.5, the seasonal amplitude of global surface ocean [H^+] is projected to increase by +73± 12 % across the CMIP6 ensemble (2080-2099 average relative to 1995-2014; Fig. 10). Concurrently, the seasonal amplitude of global surface ocean pH is projected to decrease by -10± 5 %.

500 Increases in the seasonal amplitude of [H^+] are projected in all regions but are generally highest in the high latitudes. In contrast, projected changes in the seasonal amplitude of pH can vary in sign, notably in the Southern Ocean.

The simultaneous amplification of [H^+] and attenuation of pH seasonal cycles is consistent with previous

505 assessments of CMIP5 projections, with Kwiatkowski and Orr (2018) showing [H^+] seasonal amplification of +81± 16 % and pH seasonal attenuation of -16± 7 % under RCP8.5 (2090-2099 anomalies relative to 1990-1999). Although counterintuitive, this results from the log scale of pH, which means that the seasonal amplitude of pH depends not only on the seasonal amplitude of [H^+] but also on the inverse of the annual mean [H^+]. As the projected increase in annual mean [H^+] is usually greater than the corresponding increase in the seasonal

510 amplitude of [H^+], the seasonal amplitude of pH declines as a result. Increases in the seasonal cycle of [H^+] have been shown to be primarily driven by the geochemical effect of increasing atmospheric CO_2. This affects both the seasonal amplitude of the controlling variables dissolved inorganic carbon and alkalinity, as well the sensitivity of [H^+] to seasonal changes in temperature, dissolved inorganic carbon and alkalinity (Kwiatkowski and Orr, 2018). Given the near-linear relationship between [H^+] and pCO_2 on annual timescales (Orr, 2011),

515 projected increases in the seasonal amplitude of [H^+] are in agreement with historical observations (Landschützer et al., 2018) and twenty-first century projections from CMIP5 models (McNeil and Sasse, 2016; Gallego et al., 2018) of increasing pCO_2 seasonal amplitude.

The seasonal amplitude of global surface ocean temperature is projected to increase by +0.59± 0.21 °C across

520 SSP5-8.5 (Fig. 11). Over most of the ocean, the seasonal amplitude of sea surface temperature is projected to show limited increases (< +0.5 °C). Exceptions are found in the North Atlantic, North Pacific and Southern Ocean where increases in the seasonal amplitude of SST can exceed 2 °C, and in the Arctic Ocean, where the amplitude can increase by >7 °C (>10-fold; Fig. 11).

525 The CMIP6 projections of the changing seasonal amplitude of SST under SSP5-8.5 are consistent with previous projections from the CMIP5 models (Carton et al., 2015; Alexander et al., 2018). The limited increases in SST seasonal amplitude for most of the global ocean have been attributed to greater relative shoaling of the mixed

layer depth in summer than in winter (Alexander et al., 2018). However, in the Arctic Ocean the large increase in SST seasonal amplitude is primarily due to the loss of sea ice. The seasonal melting and refreezing of sea ice

530   accounts for approximately half of the present-day seasonal Arctic Ocean net surface heat flux, buffering seasonal variability in Arctic Ocean heat content and SSTs (Serreze et al., 2007; Fig. 11). The loss of this seasonal melting/freezing cycle under high-emissions scenarios such as RCP8.5 has been shown to account for a doubling of seasonal Arctic Ocean heat content variability. Ice loss further amplifies the seasonal cycle of SSTs by increasing the seasonal cycle of net surface heat fluxes. The net downward radiative flux increases in summer

535   as albedo declines, while the net upward radiative flux increases in winter due to greater evaporative and sensible heat loss (Carton et al., 2015).

4.   Conclusions

540   The latest CMIP6 Earth system models consistently project surface ocean warming and acidification, subsurface deoxygenation and euphotic-zone nitrate reductions in the 21st century. The projected change in these ocean impact drivers is shown to increase with radiative forcing across the SSPs, highlighting the benefit of emissions reductions to upper-ocean ecosystems. The magnitude of projected warming, acidification and deoxygenation is lower in the benthic ocean, with greater model structural uncertainty relative to scenario uncertainty. However,

545   the extent of warming and acidification is still limited under lower emissions scenarios, further demonstrating the benefits of mitigation to benthic ecosystems.

In addition to changing mean-state conditions, the CMIP6 models also project changes to the seasonal cycles of temperature and carbonate chemistry under the SSPs. The seasonal amplitude of surface ocean acidity ($[H^+]$)

550   nearly doubles over the 21st century under SSP5-8.5, with a concurrent reduction in the seasonal amplitude of pH. Over the same period, the seasonal amplitude of temperature is projected to increase, particularly in the Arctic Ocean.

The CMIP6 projections of warming, acidification, deoxygenation and nutrient reduction are greater than those of

555   previous CMIP5 models under comparable radiative forcing. The enhanced acidification is a consequence of higher atmospheric CO_2 concentrations in the SSPs than their RCP analogues. The enhanced warming however reflects the greater climate sensitivity of the CMIP6 models. This increased warming results in greater increases in upper-ocean stratification, which contributes to greater reductions in euphotic nitrate and subsurface oxygen concentration.

560

Projected changes to the mean state and seasonality of physical and chemical ocean conditions are likely to present major challenges to diverse marine ecosystems from the surface ocean to abyssal depths. Potential organism stress is likely to be exacerbated by simultaneous exposure to multiple physicochemical changes, emphasising the need for extensive emissions reductions.

565

Data availability

The Earth system model output used in this study is available via the Earth System Grid Federation (https://esgf-
570   node.ipsl.upmc.fr/projects/esgf-ipsl/).

Author contribution

LK and LB conceived and designed this study. LK, LB and OT processed model outputs and performed the
analysis. All authors contributed to the ocean biogeochemistry development of the CMIP6 ESMs and/or the
575   manuscript text.

Competing interests

The authors declare that they have no conflict of interest.

580   **Disclaimer**

This article reflects only the authors' view – the funding agencies as well as their executive agencies are not
responsible for any use that may be made of the information that the article contains.

Acknowledgements

595

References

Albright, R., Caldeira, L., Hosfelt, J., Kwiatkowski, L., Maclaren, J. K., Mason, B. M., Nebuchina, Y.,
Ninokawa, A., Pongratz, J., Ricke, K. L., Rivlin, T., Schneider, K., Sesboüé, M., Shamberger, K., Silverman, J.,
Wolfe, K., Zhu, K. and Caldeira, K.: Reversal of ocean acidification enhances net coral reef calcification,
600   Nature, 531(7594), 362–365, doi:10.1038/nature17155, 2016.

Alexander, M. A., Scott, J. D., Friedland, K. D., Mills, K. E., Nye, J. A., Pershing, A. J. and Thomas, A. C.:
Projected sea surface temperatures over the 21st century: Changes in the mean, variability and extremes for large
marine ecosystem regions of Northern Oceans, Elem Sci Anth, 6(1), 9, doi:10.1525/elementa.191, 2018.

605   Andrews, O. D., Bindoff, N. L., Halloran, P. R., Ilyina, T. and Quéré, C. L.: Detecting an external influence on recent changes in oceanic oxygen using an optimal fingerprinting method, Biogeosciences, 10(3), 1799–1813, doi:https://doi.org/10.5194/bg-10-1799-2013, 2013.

Andrews, T., Gregory, J. M., Webb, M. J. and Taylor, K. E.: Forcing, feedbacks and climate sensitivity in CMIP5 coupled atmosphere   ocean climate models, Geophysical Research Letters, 39(9), doi:10.1029/2012GL051607, 2012.

610   Bates, N. R., Mathis, J. T. and Cooper, L. W.: Ocean acidification and biologically induced seasonality of carbonate mineral saturation states in the western Arctic Ocean, Journal of Geophysical Research: Oceans, 114(C11), doi:10.1029/2008JC004862, 2009.

Bates, N. R., Best, M. H. P., Neely, K., Garley, R., Dickson, A. G. and Johnson, R. J.: Detecting anthropogenic carbon dioxide uptake and ocean acidification in the North Atlantic Ocean, Biogeosciences, 9(7), 2509–2522,
615   doi:https://doi.org/10.5194/bg-9-2509-2012, 2012.

Behrenfeld, M. J., Randerson, J. T., McClain, C. R., Feldman, G. C., Los, S. O., Tucker, C. J., Falkowski, P. G., Field, C. B., Frouin, R., Esaias, W. E., Kolber, D. D. and Pollack, N. H.: Biospheric Primary Production During an ENSO Transition, Science, 291(5513), 2594–2597, doi:10.1126/science.1055071, 2001.

Behrenfeld, M. J., O'Malley, R. T., Siegel, D. A., McClain, C. R., Sarmiento, J. L., Feldman, G. C., Milligan, A.
620   J., Falkowski, P. G., Letelier, R. M. and Boss, E. S.: Climate-driven trends in contemporary ocean productivity, Nature, 444(7120), 752–755, doi:10.1038/nature05317, 2006.

Bekryaev, R. V., Polyakov, I. V. and Alexeev, V. A.: Role of Polar Amplification in Long-Term Surface Air Temperature Variations and Modern Arctic Warming, J. Climate, 23(14), 3888–3906, doi:10.1175/2010JCLI3297.1, 2010.

625   Bentsen, M., Bethke, I., Debernard, J. B., Iversen, T., Kirkevåg, A., Seland, Ø., Drange, H., Roelandt, C., Seierstad, I. A., Hoose, C. and Kristjánsson, J. E.: The Norwegian Earth System Model, NorESM1-M – Part 1: Description and basic evaluation of the physical climate, Geosci. Model Dev., 6(3), 687–720, doi:10.5194/gmd-6-687-2013, 2013.

Bindoff, Cheung, W. W. L. and J.G. Kairo, J. Arístegui, V.A. Guinder, R. Hallberg, N. Hilmi, N. Jiao, M.S.
630   Karim, L. Levin, S. O'Donoghue, S.R. Purca Cuicapusa, B. Rinkevich, T. Suga, A. Tagliabue, and P. Williamson: Changing Ocean, Marine Ecosystems, and Dependent Communities. In: IPCC Special Report on the Ocean and Cryosphere in a Changing Climate [H.-O. Pörtner, D.C. Roberts, V. Masson-Delmotte, P. Zhai, M. Tignor, E. Poloczanska, K. Mintenbeck, A. Alegría, M. Nicolai, A. Okem, J. Petzold, B. Rama, N.M. Weyer (eds.)]. In press.

635   Bindoff, N. L., Willebrand, J., Artale, V., Cazenave, A., Gregory, J. M., Gulev, S., Hanawa, K., Le Quere, C., Levitus, S., Nojiri, Y., Shum, C. K., Talley, L. D., Unnikrishnan, A. S., Josey, S. A., Tamisiea, M., Tsimplis, M. and Woodworth, P.: Observations: oceanic climate change and sea level, in Climate change 2007: the physical science basis. Contribution of Working Group I, edited by S. Solomon, D. Qin, M. Manning, Z. Chen, M. Marquis, K. B. Averyt, M. Tignor, and H. L. Miller, pp. 385–428, Cambridge University Press, Cambridge,
640   2007.

Bopp, L., Monfray, P., Aumont, O., Dufresne, J.-L., Treut, H. L., Madec, G., Terray, L. and Orr, J. C.: Potential impact of climate change on marine export production, Global Biogeochemical Cycles, 15(1), 81–99, doi:10.1029/1999GB001256, 2001.

Bopp, L., Resplandy, L., Orr, J. C., Doney, S. C., Dunne, J. P., Gehlen, M., Halloran, P., Heinze, C., Ilyina, T.,
645 Séférian, R., Tjiputra, J. and Vichi, M.: Multiple stressors of ocean ecosystems in the 21st century: projections with CMIP5 models, Biogeosciences, 10(10), 6225–6245, doi:10.5194/bg-10-6225-2013, 2013.

Bopp, L., Resplandy, L., Untersee, A., Le Mezo, P. and Kageyama, M.: Ocean (de)oxygenation from the Last Glacial Maximum to the twenty-first century: insights from Earth System models, Philos Trans A Math Phys Eng Sci, 375(2102), doi:10.1098/rsta.2016.0323, 2017.

650 Boucher, O,. Servonnat, J., Albright, A. L., Aumont, O., Balkanski, Y., Bastrikov, V., Bekki, S., Bonnet, R., Bony, S., Bopp, L., Braconnot, P., Brockmann, P., Cadule, P., Caubel, A., Cheruy, F., Cozic, A., Cugnet, D., D'Andrea, F., Davini, P., de Lavergne, C., Denvil, S., Deshayes, J., Devilliers, M., Ducharne, A., Dufresne, J.-L., Dupont, E., Éthé, C., Fairhead, L., Falletti, L., Foujols, M.-A., Gardoll, S., Gastineau, G., Ghattas, J., Grandpeix, J.-Y., Guenet, B., Guez, L., Guilyardi, E., Guimberteau, M., Hauglustaine, D., Hourdin, F. Idelkadi,
655 A., Joussaume, S., Kageyama, M., Khodri, M., Krinner, G., Lebas, N., Levavasseur, G., Lévy, C., Li, L., Lott, F., Lurton, T., Luyssaert, S., Madec, G., Madeleine, J.-B., Maignan, F., Marchand, M., Marti, O., Mellul, L., Meurdesoif, Y., Mignot, J., Musat, I., Ottlé, C., Peylin, P., Planton, Y., Polcher, J., Rio, C., Rousset, C., Sepulchre, P., Sima, A., Swingedouw, D., Thi éblemont, R., Traoré, A.-K., Vancoppenolle, M., Vial, J., Vialard, J., Viovy, N., Vuichard, N.: Presentation and evaluation of the IPSL-CM6A-LR climate model, Journal of
660 Advances in Modeling Earth Systems, in review.

Breitburg, D., Levin, L. A., Oschlies, A., Grégoire, M., Chavez, F. P., Conley, D. J., Garçon, V., Gilbert, D., Gutiérrez, D., Isensee, K., Jacinto, G. S., Limburg, K. E., Montes, I., Naqvi, S. W. A., Pitcher, G. C., Rabalais, N. N., Roman, M. R., Rose, K. A., Seibel, B. A., Telszewski, M., Yasuhara, M. and Zhang, J.: Declining oxygen in the global ocean and coastal waters, Science, 359(6371), doi:10.1126/science.aam7240, 2018.

665 Byrne, R. H., Mecking, S., Feely, R. A. and Liu, X.: Direct observations of basin-wide acidification of the North Pacific Ocean, Geophysical Research Letters, 37(2), doi:10.1029/2009GL040999, 2010.

Cabré, A., Marinov, I. and Leung, S.: Consistent global responses of marine ecosystems to future climate change across the IPCC AR5 earth system models, Clim Dyn, 45(5–6), 1253–1280, doi:10.1007/s00382-014-2374-3, 2014.

670 Cabré, A., Marinov, I., Bernardello, R. and Bianchi, D.: Oxygen minimum zones in the tropical Pacific across CMIP5 models: mean state differences and climate change trends, Biogeosciences, 12(18), 5429–5454, doi:10.5194/bg-12-5429-2015, 2015.

Cagnazzo, C., Manzini, E., Fogli, P. G., Vichi, M. and Davini, P.: Role of stratospheric dynamics in the ozone–carbon connection in the Southern Hemisphere, Clim Dyn, 41(11–12), 3039–3054, doi:10.1007/s00382-013-
675 1745-5, 2013.

Capotondi, A., Alexander, M. A., Bond, N. A., Curchitser, E. N. and Scott, J. D.: Enhanced upper ocean stratification with climate change in the CMIP3 models, Journal of Geophysical Research: Oceans, 117(C4), doi:10.1029/2011JC007409, 2012.

Carton, J. A., Ding, Y. and Arrigo, K. R.: The seasonal cycle of the Arctic Ocean under climate change, Geophysical Research Letters, 42(18), 7681–7686, doi:10.1002/2015GL064514, 2015.

Cheng, L., Abraham, J., Hausfather, Z. and Trenberth, K. E.: How fast are the oceans warming?, Science, 363(6423), 128–129, doi:10.1126/science.aav7619, 2019.

Cheng, W., Chiang, J. C. H. and Zhang, D.: Atlantic Meridional Overturning Circulation (AMOC) in CMIP5 Models: RCP and Historical Simulations, J. Climate, 26(18), 7187–7197, doi:10.1175/JCLI-D-12-00496.1, 2013.

Chust, G., Allen, J. I., Bopp, L., Schrum, C., Holt, J., Tsiaras, K., Zavatarelli, M., Chifflet, M., Cannaby, H., Dadou, I., Daewel, U., Wakelin, S. L., Machu, E., Pushpadas, D., Butenschon, M., Artioli, Y., Petihakis, G., Smith, C., Garçon, V., Goubanova, K., Le Vu, B., Fach, B. A., Salihoglu, B., Clementi, E. and Irigoien, X.: Biomass changes and trophic amplification of plankton in a warmer ocean, Glob Change Biol, 20(7), 2124–2139, doi:10.1111/gcb.12562, 2014.

Cocco, V., Joos, F., Steinacher, M., Frölicher, T. L., Bopp, L., Dunne, J., Gehlen, M., Heinze, C., Orr, J., Oschlies, A., Schneider, B., Segschneider, J. and Tjiputra, J.: Oxygen and indicators of stress for marine life in multi-model global warming projections, Biogeosciences, 10(3), 1849–1868, doi:info:doi:10.5194/bg-10-1849-2013, 2013.

Collins, W. J., Bellouin, N., Doutriaux-Boucher, M., Gedney, N., Halloran, P., Hinton, T., Hughes, J., Jones, C. D., Joshi, M., Liddicoat, S., Martin, G., O'Connor, F., Rae, J., Senior, C., Sitch, S., Totterdell, I., Wiltshire, A. and Woodward, S.: Development and evaluation of an Earth-System model – HadGEM2, Geosci. Model Dev., 4(4), 1051–1075, doi:10.5194/gmd-4-1051-2011, 2011.

Deutsch, C., Brix, H., Ito, T., Frenzel, H. and Thompson, L.: Climate-Forced Variability of Ocean Hypoxia, Science, 333(6040), 336–339, doi:10.1126/science.1202422, 2011.

Deutsch, C., Ferrel, A., Seibel, B., Pörtner, H.-O. and Huey, R. B.: Climate change tightens a metabolic constraint on marine habitats, Science, 348(6239), 1132–1135, doi:10.1126/science.aaa1605, 2015.

Doney, S. C., Fabry, V. J., Feely, R. A. and Kleypas, J. A.: Ocean Acidification: The Other CO2 Problem, Annual Review of Marine Science, 1, 169–192, doi:10.1146/annurev.marine.010908.163834, 2009.

Dore, J. E., Lukas, R., Sadler, D. W., Church, M. J. and Karl, D. M.: Physical and biogeochemical modulation of ocean acidification in the central North Pacific, PNAS, 106(30), 12235–12240, doi:10.1073/pnas.0906044106, 2009.

Drijfhout, S., van Oldenborgh, G. J. and Cimatoribus, A.: Is a Decline of AMOC Causing the Warming Hole above the North Atlantic in Observed and Modeled Warming Patterns?, J. Climate, 25(24), 8373–8379, doi:10.1175/JCLI-D-12-00490.1, 2012.

Dufresne, J.-L., Foujols, M.-A., Denvil, S., Caubel, A., Marti, O., Aumont, O., Balkanski, Y., Bekki, S., Bellenger, H., Benshila, R., Bony, S., Bopp, L., Braconnot, P., Brockmann, P., Cadule, P., Cheruy, F., Codron, F., Cozic, A., Cugnet, D., Noblet, N., Duvel, J.-P., Ethé, C., Fairhead, L., Fichefet, T., Flavoni, S., Friedlingstein, P., Grandpeix, J.-Y., Guez, L., Guilyardi, E., Hauglustaine, D., Hourdin, F., Idelkadi, A., Ghattas, J., Joussaume, S., Kageyama, M., Krinner, G., Labetoulle, S., Lahellec, A., Lefebvre, M.-P., Lefevre, F., Levy, C., Li, Z. X.,

Lloyd, J., Lott, F., Madec, G., Mancip, M., Marchand, M., Masson, S., Meurdesoif, Y., Mignot, J., Musat, I., Parouty, S., Polcher, J., Rio, C., Schulz, M., Swingedouw, D., Szopa, S., Talandier, C., Terray, P., Viovy, N. and Vuichard, N.: Climate change projections using the IPSL-CM5 Earth System Model: from CMIP3 to CMIP5, Clim Dyn, 40(9–10), 2123–2165, doi:10.1007/s00382-012-1636-1, 2013.

720   Dunne, J. P., John, J. G., Adcroft, A. J., Griffies, S. M., Hallberg, R. W., Shevliakova, E., Stouffer, R. J., Cooke, W., Dunne, K. A., Harrison, M. J., Krasting, J. P., Malyshev, S. L., Milly, P. C. D., Phillipps, P. J., Sentman, L. T., Samuels, B. L., Spelman, M. J., Winton, M., Wittenberg, A. T. and Zadeh, N.: GFDL's ESM2 Global Coupled Climate–Carbon Earth System Models. Part I: Physical Formulation and Baseline Simulation Characteristics, J. Climate, 25(19), 6646–6665, doi:10.1175/JCLI-D-11-00560.1, 2012.

725   Dunne, J. P., Horowitz, L. W. , Adcroft, A. J., Ginoux, P. , Held, I. M., John, J. G., Krasting, J. P., Malyshev, S., Naik, V., Paulot, F., Shevliakova, E., Stock, C. A., Zadeh, N., Balaji, V., Blanton, C., Dunne, K. A., Dupuis, C., Durachta, J., Dussin, R., Gauthier, P. P. G., Griffies, S. M., Guo, H., Hallberg, R. W., Harrison, M., He, J., Hurlin, W., McHugh, C., Menzel, R., Milly, P. C. D., Nikonov, S., Paynter, D. J., Ploshay, J., Radhakrishnan, A., Rand, K., Reichl, B. G., Robinson, T., Schwarzkopf, D. M., Sentman, L. A., Underwood, S., Vahlenkamp, 730   H., Winton, M., Wittenberg, A. T., Wyman, B., Zeng, Y., and Zhao, M.: The GFDL Earth System Model version 4.1 (GFDL-ESM4.1): Model description and simulation characteristics. Journal of Advances in Modeling Earth Systems. 2019MS002008, in review.

Dunne, J. P., Bociu, I., Bronselaer, B., Guo, H., John, J. G., Krasting, J. P., Stock, C. A., Winton, M., and Zadeh, N.: Simple Global Ocean Biogeochemistry with Light, Iron, Nutrients and Gas version 2 (BLINGv2): Model 735   description and simulation characteristics in GFDL's CM4.0. Journal of Advances in Modeling Earth Systems, 2019MS002008, in review.

Eppley, R. W.: Temperature and phytoplankton growth in the sea, Fishery bulletin, 70(4), 1063–85, 1972.

Eyring, V., Bony, S., Meehl, G. A., Senior, C. A., Stevens, B., Stouffer, R. J. and Taylor, K. E.: Overview of the Coupled Model Intercomparison Project Phase 6 (CMIP6) experimental design and organization, Geosci. Model 740   Dev., 9(5), 1937–1958, doi:10.5194/gmd-9-1937-2016, 2016.

Freeman, N. M., Lovenduski, N. S., Munro, D. R., Krumhardt, K. M., Lindsay, K., Long, M. C., and Maclennan, M.: The variable and changing Southern Ocean Silicate Front: Insights from the CESM Large Ensemble, Global Biogeochem. Cycles, 32, 752-768, doi:10.1029/2017GB005816, 2018.

Forster, P. M., Maycock, A. C., McKenna, C. M. and Smith, C. J.: Latest climate models confirm need for 745   urgent mitigation, Nat. Clim. Chang., 1–4, doi:10.1038/s41558-019-0660-0, 2019.

Frölicher, T. L., Sarmiento, J. L., Paynter, D. J., Dunne, J. P., Krasting, J. P. and Winton, M.: Dominance of the Southern Ocean in Anthropogenic Carbon and Heat Uptake in CMIP5 Models, J. Climate, 28(2), 862–886, doi:10.1175/JCLI-D-14-00117.1, 2014.

Frölicher, T. L., Rodgers, K. B., Stock, C. A. and Cheung, W. W. L.: Sources of uncertainties in 21st century 750   projections of potential ocean ecosystem stressors, Global Biogeochem. Cycles, 30(8), 2015GB005338, doi:10.1002/2015GB005338, 2016.

Frölicher, T. L., Fischer, E. M. and Gruber, N.: Marine heatwaves under global warming, Nature, 560(7718), 360–364, doi:10.1038/s41586-018-0383-9, 2018.

755   Fu, W., Randerson, J. T. and Moore, J. K.: Climate change impacts on net primary production (NPP) and export
        production (EP) regulated by increasing stratification and phytoplankton community structure in the CMIP5
        models, Biogeosciences, 13(18), 5151–5170, doi:https://doi.org/10.5194/bg-13-5151-2016, 2016.

        Gallego, M. A., Timmermann, A., Friedrich, T. and Zeebe, R. E.: Drivers of future seasonal cycle changes in
        oceanic pCO$_2$, Biogeosciences, 15(17), 5315–5327, doi:https://doi.org/10.5194/bg-15-5315-2018, 2018.

760   Garrabou, J., Coma, R., Bensoussan, N., Bally, M., Chevaldonné, P., Cigliano, M., Diaz, D., Harmelin, J. G.,
        Gambi, M. C., Kersting, D. K., Ledoux, J. B., Lejeusne, C., Linares, C., Marschal, C., Pérez, T., Ribes, M.,
        Romano, J. C., Serrano, E., Teixido, N., Torrents, O., Zabala, M., Zuberer, F. and Cerrano, C.: Mass mortality in
        Northwestern Mediterranean rocky benthic communities: effects of the 2003 heat wave, Global Change Biology,
        15(5), 1090–1103, doi:10.1111/j.1365-2486.2008.01823.x, 2009.

        Gattuso, J.-P. and Buddemeier, R. W.: Ocean biogeochemistry: Calcification and CO2, Nature, 407(6802), 311–
765   314, 2000.

        Gattuso, J.-P. and Hansson, L.: Ocean Acidification, OUP Oxford., 2011.

        Gehlen, M., Séférian, R., Jones, D. O. B., Roy, T., Roth, R., Barry, J. P., Bopp, L., Doney, S. C., Dunne, J. P.,
        Heinze, C., Joos, F., Orr, J. C., Resplandy, L., Segschneider, J. and Tjiputra, J.: Projected pH reductions by 2100
        might put deep North Atlantic biodiversity at risk, 1726-4170, doi:10.5194/bg-11-6955-2014, 2014.

770   Gent, P. R., Danabasoglu, G., Donner, L. J., Holland, M. M., Hunke, E. C., Jayne, S. R., Lawrence, D. M.,
        Neale, R. B., Rasch, P. J., Vertenstein, M., Worley, P. H., Yang, Z.-L. and Zhang, M.: The Community Climate
        System Model Version 4, J. Climate, 24(19), 4973–4991, doi:10.1175/2011JCLI4083.1, 2011.

        Giorgetta, M. A., Jungclaus, J., Reick, C. H., Legutke, S., Bader, J., Böttinger, M., Brovkin, V., Crueger, T.,
        Esch, M., Fieg, K., Glushak, K., Gayler, V., Haak, H., Hollweg, H.-D., Ilyina, T., Kinne, S., Kornblueh, L.,
775   Matei, D., Mauritsen, T., Mikolajewicz, U., Mueller, W., Notz, D., Pithan, F., Raddatz, T., Rast, S., Redler, R.,
        Roeckner, E., Schmidt, H., Schnur, R., Segschneider, J., Six, K. D., Stockhause, M., Timmreck, C., Wegner, J.,
        Widmann, H., Wieners, K.-H., Claussen, M., Marotzke, J. and Stevens, B.: Climate and carbon cycle changes
        from 1850 to 2100 in MPI-ESM simulations for the Coupled Model Intercomparison Project phase 5, J. Adv.
        Model. Earth Syst., 5(3), 572–597, doi:10.1002/jame.20038, 2013.

780   Gregory, B., Christophe, L. and Martin, E.: Rapid biogeographical plankton shifts in the North Atlantic Ocean,
        Global Change Biology, 15(7), 1790–1803, doi:10.1111/j.1365-2486.2009.01848.x, 2009.

        Gregory, J. M., Dixon, K. W., Stouffer, R. J., Weaver, A. J., Driesschaert, E., Eby, M., Fichefet, T., Hasumi, H.,
        Hu, A., Jungclaus, J. H., Kamenkovich, I. V., Levermann, A., Montoya, M., Murakami, S., Nawrath, S., Oka, A.,
        Sokolov, A. P. and Thorpe, R. B.: A model intercomparison of changes in the Atlantic thermohaline circulation
785   in response to increasing atmospheric CO2 concentration, Geophysical Research Letters, 32(12),
        doi:10.1029/2005GL023209, 2005.

        Gruber, N.: The Dynamics of the Marine Nitrogen Cycle and its Influence on Atmospheric CO2 Variations, in
        The Ocean Carbon Cycle and Climate, edited by M. Follows and T. Oguz, pp. 97–148, Springer Netherlands,
        Dordrecht., 2004.

790   Gruber, N., Clement, D., Carter, B. R., Feely, R. A., van Heuven, S., Hoppema, M., Ishii, M., Key, R. M.,
       Kozyr, A., Lauvset, S. K., Lo Monaco, C., Mathis, J. T., Murata, A., Olsen, A., Perez, F. F., Sabine, C. L.,
       Tanhua, T., and Wanninkhof, R.: The oceanic sink for anthropogenic CO2 from 1994 to 2007, Science, 363,
       1193–1199, https://doi.org/10.1126/science.aau5153, 2019.

       Gunderson, A. R., Armstrong, E. J. and Stillman, J. H.: Multiple Stressors in a Changing World: The Need for
795   an Improved Perspective on Physiological Responses to the Dynamic Marine Environment, Annual Review of
       Marine Science, 8(1), 357–378, doi:10.1146/annurev-marine-122414-033953, 2016.

       Hajima, T., Watanabe, M., Yamamoto, A., Tatebe, H., Noguchi, M. A., Abe, M., Ohgaito, R., Ito, A., Yamazaki,
       D., Okajima, H., Ito, A., Takata, K., Ogochi, K., Watanabe, S., and Kawamiya, M.: Description of the MIROC-
       ES2L Earth system model and evaluation of its climate–biogeochemical processes and feedback, Geosci. Model
800   Dev. Discuss., doi:10.5194/gmd-2019-275, in review, 2019.

       Harvey, B. P., Gwynn   Jones, D. and Moore, P. J.: Meta-analysis reveals complex marine biological responses
       to the interactive effects of ocean acidification and warming, Ecology and Evolution, 3(4), 1016–1030,
       doi:10.1002/ece3.516, 2013.

       Held, I. M., Guo, H., Adcroft, A., Dunne, J. P., Horowitz, L. W., Krasting, J., Shevliakova, E., Winton, M.,
805   Zhao, M., Bushuk, M., Wittenberg, A. T., Wyman, B., Xiang, B., Zhang, R., Anderson, W., Balaji, V., Donner,
       L., Dunne, K., Durachta, J., Gauthier, P. P. G., Ginoux, P., Golaz, J.-C., Griffies, S. M., Hallberg, R., Harris, L.,
       Harrison, M., Hurlin, W., John, J., Lin, P., Lin, S.-J., Malyshev, S., Menzel, R., Milly, P. C. D., Ming, Y., Naik,
       V., Paynter, D., Paulot, F., Rammaswamy, V., Reichl, B., Robinson, T., Rosati, A., Seman, C., Silvers, L. G.,
       Underwood, S. and Zadeh, N.: Structure and Performance of GFDL's CM4.0 Climate Model, Journal of
810   Advances in Modeling Earth Systems, 11(11), 3691–3727, doi:10.1029/2019MS001829, 2019.

       Helm, K. P., Bindoff, N. L. and Church, J. A.: Observed decreases in oxygen content of the global ocean,
       Geophysical Research Letters, 38(23), doi:10.1029/2011GL049513, 2011.

       Hobday, A. J., Alexander, L. V., Perkins, S. E., Smale, D. A., Straub, S. C., Oliver, E. C. J., Benthuysen, J. A.,
       Burrows, M. T., Donat, M. G., Feng, M., Holbrook, N. J., Moore, P. J., Scannell, H. A., Sen Gupta, A. and
815   Wernberg, T.: A hierarchical approach to defining marine heatwaves, Progress in Oceanography, 141, 227–238,
       doi:10.1016/j.pocean.2015.12.014, 2016.

       Ito, T., Minobe, S., Long, M. C., and Deutsch, C. (2017), Upper ocean O_2 trends: 1958–2015, *Geophys. Res.
       Lett.*, 44, 4214– 4223, doi:10.1002/2017GL073613.

       Keeling, R. F., Körtzinger, A. and Gruber, N.: Ocean Deoxygenation in a Warming World, Annual Review of
820   Marine Science, 2(1), 199–229, doi:10.1146/annurev.marine.010908.163855, 2010.

       Khatiwala, S., Primeau, F. and Hall, T.: Reconstruction of the history of anthropogenic CO 2 concentrations in
       the ocean, Nature, 462(7271), 346–349, doi:10.1038/nature08526, 2009.

       Khatiwala, S., Tanhua, T., Mikaloff Fletcher, S., Gerber, M., Doney, S. C., Graven, H. D., Gruber, N.,
       McKinley, G. A., Murata, A., Ríos, A. F. and Sabine, C. L.: Global ocean storage of anthropogenic carbon,
825   Biogeosciences, 10(4), 2169–2191, doi:https://doi.org/10.5194/bg-10-2169-2013, 2013.

Knutti, R., Masson, D. and Gettelman, A.: Climate model genealogy: Generation CMIP5 and how we got there, Geophysical Research Letters, 1194–1199, doi:10.1002/grl.50256@10.1002/(ISSN)1944-8007.GRLCMIP5, 2015.

830 Kriegler, E., Bauer, N., Popp, A., Humpenöder, F., Leimbach, M., Strefler, J., Baumstark, L., Bodirsky, B. L., Hilaire, J., Klein, D., Mouratiadou, I., Weindl, I., Bertram, C., Dietrich, J.-P., Luderer, G., Pehl, M., Pietzcker, R., Piontek, F., Lotze-Campen, H., Biewald, A., Bonsch, M., Giannousakis, A., Kreidenweis, U., Müller, C., Rolinski, S., Schultes, A., Schwanitz, J., Stevanovic, M., Calvin, K., Emmerling, J., Fujimori, S. and Edenhofer, O.: Fossil-fueled development (SSP5): An energy and resource intensive scenario for the 21st century, Global Environmental Change, 42, 297–315, doi:10.1016/j.gloenvcha.2016.05.015, 2017.

835 Kroeker, K. J., Kordas, R. L., Crim, R. N. and Singh, G. G.: Meta-analysis reveals negative yet variable effects of ocean acidification on marine organisms, Ecology Letters, 13(11), 1419–1434, doi:10.1111/j.1461-0248.2010.01518.x, 2010.

Kroeker, K. J., Micheli, F. and Gambi, M. C.: Ocean acidification causes ecosystem shifts via altered competitive interactions, Nature Clim Change, 3(2), 156–159, doi:10.1038/nclimate1680, 2013.

840 Krumhardt, K. M., Lovenduski, N. S., Long, M. C., and Lindsay, K.: Avoidable impacts of ocean warming on marine primary production: Insights from the CESM ensembles, Global Biogeochem. Cycles, 31, 114-133, doi:10.1002/2016GB005528, 2016.

Kwiatkowski, L. and Orr, J. C.: Diverging seasonal extremes for ocean acidification during the twenty-first century, Nature Climate Change, 8(2), 141–145, doi:10.1038/s41558-017-0054-0, 2018.

845 Kwiatkowski, L., Gaylord, B., Hill, T., Hosfelt, J., Kroeker, K. J., Nebuchina, Y., Ninokawa, A., Russell, A. D., Rivest, E. B., Sesboüé, M. and Caldeira, K.: Nighttime dissolution in a temperate coastal ocean ecosystem increases under acidification, Scientific Reports, 6, 22984, doi:10.1038/srep22984, 2016.

Kwiatkowski, L., Bopp, L., Aumont, O., Ciais, P., Cox, P. M., Laufkötter, C., Li, Y. and Séférian, R.: Emergent constraints on projections of declining primary production in the tropical oceans, Nature Clim. Change, 7(5), 850 355–358, doi:10.1038/nclimate3265, 2017.

Kwiatkowski, L., Aumont, O. and Bopp, L.: Consistent trophic amplification of marine biomass declines under climate change, Global Change Biology, doi:10.1111/gcb.14468, 2018.

Landschützer, P., Gruber, N., Bakker, D. C. E., Stemmler, I. and Six, K. D.: Strengthening seasonal marine CO_2 variations due to increasing atmospheric CO_2, Nature Climate Change, 8(2), 146, doi:10.1038/s41558-017-855 0057-x, 2018.

Langenbuch, M., Bock, C., Leibfritz, D. and Pörtner, H. O.: Effects of environmental hypercapnia on animal physiology: A 13C NMR study of protein synthesis rates in the marine invertebrate Sipunculus nudus, Comparative Biochemistry and Physiology Part A: Molecular & Integrative Physiology, 144(4), 479–484, doi:10.1016/j.cbpa.2006.04.017, 2006.

860 Laufkötter, C., Vogt, M., Gruber, N., Aita-Noguchi, M., Aumont, O., Bopp, L., Buitenhuis, E., Doney, S. C., Dunne, J., Hashioka, T., Hauck, J., Hirata, T., John, J., Le Quéré, C., Lima, I. D., Nakano, H., Séférian, R.,

Totterdell, I., Vichi, M. and Völker, C.: Drivers and uncertainties of future global marine primary production in marine ecosystem models, Biogeosciences, 12(23), 6955–6984, doi:10.5194/bg-12-6955-2015, 2015.

Lauvset, S. K., Gruber, N., Landschützer, P., Olsen, A., and Tjiputra, J.: Trends and drivers in global surface
865 ocean pH over the past 3 decades, Biogeosciences, 12, 1285-1298, doi:10.5194/bg-12-1285-2015, 2015.

Levin, L. A. and Bris, N. L.: The deep ocean under climate change, Science, 350(6262), 766–768, doi:10.1126/science.aad0126, 2015.

Lotze, H. K., Tittensor, D. P., Bryndum-Buchholz, A., Eddy, T. D., Cheung, W. W. L., Galbraith, E. D., Barange, M., Barrier, N., Bianchi, D., Blanchard, J. L., Bopp, L., Büchner, M., Bulman, C. M., Carozza, D. A.,
870 Christensen, V., Coll, M., Dunne, J. P., Fulton, E. A., Jennings, S., Jones, M. C., Mackinson, S., Maury, O., Niiranen, S., Oliveros-Ramos, R., Roy, T., Fernandes, J. A., Schewe, J., Shin, Y.-J., Silva, T. A. M., Steenbeek, J., Stock, C. A., Verley, P., Volkholz, J., Walker, N. D. and Worm, B.: Global ensemble projections reveal trophic amplification of ocean biomass declines with climate change, PNAS, 116(26), 12907–12912, doi:10.1073/pnas.1900194116, 2019.

875 Lovenduski, N. S., McKinley, G. A., Fay, A. R., Lindsay, K., and Long, M. S.: Partitioning uncertainty in ocean carbon uptake projections: Internal variability, emission scenario, and model structure, Global Biogeochem. Cycles, 30, 1276-1287, doi:10.1002/2016GB005426, 2016.

Lovenduski, N. S., and Bonan, G. B.: Reducing uncertainty in projections of terrestrial carbon uptake, Env. Res. Lett, 12, 044020, doi:10.1088/1748-9326/aa66b8, 2017.

880 Masson, D. and Knutti, R.: Climate model genealogy, Geophysical Research Letters, 38(8), doi:10.1029/2011GL046864, 2011.

Mauritsen, T., Bader, J., Becker, T., Behrens, J., Bittner, M., Brokopf, R., et al. (2019). Developments in the MPI-M Earth System Model version 1.2 (MPI-ESM1.2) and its response to increasing CO2. Journal of Advances in Modeling Earth Systems, 11, 998–1038. https://doi.org/10.1029/2018MS001400

885 McBryan, T. L., Anttila, K., Healy, T. M. and Schulte, P. M.: Responses to Temperature and Hypoxia as Interacting Stressors in Fish: Implications for Adaptation to Environmental Change, Integr Comp Biol, 53(4), 648–659, doi:10.1093/icb/ict066, 2013.

McNeil, B. I. and Matear, R. J.: Climate change feedbacks on future oceanic acidification, Tellus B: Chemical and Physical Meteorology, 59(2), 191–198, doi:10.1111/j.1600-0889.2006.00241, 2007.

890 McNeil, B. I. and Sasse, T. P.: Future ocean hypercapnia driven by anthropogenic amplification of the natural CO2 cycle, Nature, 529(7586), 383–386, doi:10.1038/nature16156, 2016.

Meinshausen, M., Smith, S. J., Calvin, K., Daniel, J. S., Kainuma, M. L. T., Lamarque, J.-F., Matsumoto, K., Montzka, S. A., Raper, S. C. B., Riahi, K., Thomson, A., Velders, G. J. M. and van Vuuren, D. P. P.: The RCP greenhouse gas concentrations and their extensions from 1765 to 2300, Climatic Change, 109(1), 213,
895 doi:10.1007/s10584-011-0156-z, 2011.

Meinshausen, M., Nicholls, Z., Lewis, J., Gidden, M. J., Vogel, E., Freund, M., Beyerle, U., Gessner, C., Nauels, A., Bauer, N., Canadell, J. G., Daniel, J. S., John, A., Krummel, P., Luderer, G., Meinshausen, N., Montzka, S. A., Rayner, P., Reimann, S., Smith, S. J., Berg, M. van den, Velders, G. J. M., Vollmer, M. and Wang, H. J.: The

SSP greenhouse gas concentrations and their extensions to 2500, Geoscientific Model Development Discussions,
900   1–77, doi:https://doi.org/10.5194/gmd-2019-222, 2019.

Menary, M. B. and Wood, R. A.: An anatomy of the projected North Atlantic warming hole in CMIP5 models,
Clim Dyn, 50(7), 3063–3080, doi:10.1007/s00382-017-3793-8, 2018.

Moore, J. K., Fu, W., Primeau, F., Britten, G. L., Lindsay, K., Long, M., Doney, S. C., Mahowald, N., Hoffman,
F. and Randerson, J. T.: Sustained climate warming drives declining marine biological productivity, Science,
905   359(6380), 1139–1143, doi:10.1126/science.aao6379, 2018.

Mora, C., Wei, C.-L., Rollo, A., Amaro, T., Baco, A. R., Billett, D., Bopp, L., Chen, Q., Collier, M., Danovaro,
R., Gooday, A. J., Grupe, B. M., Halloran, P. R., Ingels, J., Jones, D. O. B., Levin, L. A., Nakano, H., Norling,
K., Ramirez-Llodra, E., Rex, M., Ruhl, H. A., Smith, C. R., Sweetman, A. K., Thurber, A. R., Tjiputra, J. F.,
Usseglio, P., Watling, L., Wu, T. and Yasuhara, M.: Biotic and Human Vulnerability to Projected Changes in
910   Ocean Biogeochemistry over the 21st Century, PLOS Biology, 11(10), e1001682,
doi:10.1371/journal.pbio.1001682, 2013.

Munday, P. L., Dixson, D. L., Donelson, J. M., Jones, G. P., Pratchett, M. S., Devitsina, G. V. and Døving, K.
B.: Ocean acidification impairs olfactory discrimination and homing ability of a marine fish, PNAS, 106(6),
1848–1852, doi:10.1073/pnas.0809996106, 2009.

915   Müller, W. A., Jungclaus, J. H.,Mauritsen, T., Baehr, J., Bittner, M., Budich, R., et al. (2018). A higher-
resolution version of the Max Planck Institute Earth System Model (MPI-ESM1.2-HR). Journal of Advances in
Modeling Earth Systems, 10, 1383–1413. https://doi.org/10.1029/2017MS001217

O'Neill, B. C., Tebaldi, C., Vuuren, D. P. van, Eyring, V., Friedlingstein, P., Hurtt, G., Knutti, R., Kriegler, E.,
Lamarque, J.-F., Lowe, J., Meehl, G. A., Moss, R., Riahi, K. and Sanderson, B. M.: The Scenario Model
920   Intercomparison Project (ScenarioMIP) for CMIP6, Geoscientific Model Development, 9(9), 3461–3482,
doi:https://doi.org/10.5194/gmd-9-3461-2016, 2016.

Orr, J. C.: Recent and future changes in ocean carbonate chemistry, in Ocean acidification, vol. 1, pp. 41–66.,
2011.

Orr, J. C., Fabry, V. J., Aumont, O., Bopp, L., Doney, S. C., Feely, R. A., Gnanadesikan, A., Gruber, N., Ishida,
925   A., Joos, F., Key, R. M., Lindsay, K., Maier-Reimer, E., Matear, R., Monfray, P., Mouchet, A., Najjar, R. G.,
Plattner, G.-K., Rodgers, K. B., Sabine, C. L., Sarmiento, J. L., Schlitzer, R., Slater, R. D., Totterdell, I. J.,
Weirig, M.-F., Yamanaka, Y. and Yool, A.: Anthropogenic ocean acidification over the twenty-first century and
its impact on calcifying organisms, Nature, 437(7059), 681–686, doi:10.1038/nature04095, 2005.

Orr, J. C., Najjar, R. G., Aumont, O., Bopp, L., Bullister, J. L., Danabasoglu, G., Doney, S. C., Dunne, J. P.,
930   Dutay, J.-C., Graven, H., Griffies, S. M., John, J. G., Joos, F., Levin, I., Lindsay, K., Matear, R. J., McKinley, G.
A., Mouchet, A., Oschlies, A., Romanou, A., Schlitzer, R., Tagliabue, A., Tanhua, T. and Yool, A.:
Biogeochemical protocols and diagnostics for the CMIP6 Ocean Model Intercomparison Project (OMIP),
Geosci. Model Dev., 10(6), 2169–2199, doi:10.5194/gmd-10-2169-2017, 2017.

Oschlies, A., Brandt, P., Stramma, L. and Schmidtko, S.: Drivers and mechanisms of ocean deoxygenation,
935   Nature Geosci, 11(7), 467–473, doi:10.1038/s41561-018-0152-2, 2018.

24

Pithan, F. and Mauritsen, T.: Arctic amplification dominated by temperature feedbacks in contemporary climate models, Nature Geosci, 7(3), 181–184, doi:10.1038/ngeo2071, 2014.

Pörtner, H.-O.: Ecosystem effects of ocean acidification in times of ocean warming: a physiologists view, Marine Ecology Progress Series, 373, 203–217, doi:10.3354/meps07768, 2008.

940 Pörtner, H.-O.: Oxygen- and capacity-limitation of thermal tolerance: a matrix for integrating climate-related stressor effects in marine ecosystems, Journal of Experimental Biology, 213(6), 881–893, doi:10.1242/jeb.037523, 2010.

Resplandy, L., Bopp, L., Orr, J. C. and Dunne, J. P.: Role of mode and intermediate waters in future ocean acidification: Analysis of CMIP5 models, Geophysical Research Letters, 40(12), 3091–3095,
945 doi:10.1002/grl.50414, 2013.

Riahi, K., van Vuuren, D. P., Kriegler, E., Edmonds, J., O'Neill, B. C., Fujimori, S., Bauer, N., Calvin, K., Dellink, R., Fricko, O., Lutz, W., Popp, A., Cuaresma, J. C., Kc, S., Leimbach, M., Jiang, L., Kram, T., Rao, S., Emmerling, J., Ebi, K., Hasegawa, T., Havlik, P., Humpenöder, F., Da Silva, L. A., Smith, S., Stehfest, E., Bosetti, V., Eom, J., Gernaat, D., Masui, T., Rogelj, J., Strefler, J., Drouet, L., Krey, V., Luderer, G., Harmsen,
950 M., Takahashi, K., Baumstark, L., Doelman, J. C., Kainuma, M., Klimont, Z., Marangoni, G., Lotze-Campen, H., Obersteiner, M., Tabeau, A. and Tavoni, M.: The Shared Socioeconomic Pathways and their energy, land use, and greenhouse gas emissions implications: An overview, Global Environmental Change, 42, 153–168, doi:10.1016/j.gloenvcha.2016.05.009, 2017.

Sabine, C. L., Feely, R. A., Gruber, N., Key, R. M., Lee, K., Bullister, J. L., Wanninkhof, R., Wong, C. S.,
955 Wallace, D. W. R., Tilbrook, B., Millero, F. J., Peng, T.-H., Kozyr, A., Ono, T. and Rios, A. F.: The Oceanic Sink for Anthropogenic CO2, Science, 305(5682), 367–371, doi:10.1126/science.1097403, 2004.

Sanderson, B. M., Knutti, R. and Caldwell, P.: A Representative Democracy to Reduce Interdependency in a Multimodel Ensemble, J. Climate, 28(13), 5171–5194, doi:10.1175/JCLI-D-14-00362.1, 2015.

Sarmiento, J. L., Slater, R., Barber, R., Bopp, L., Doney, S. C., Hirst, A. C., Kleypas, J., Matear, R.,
960 Mikolajewicz, U., Monfray, P., Soldatov, V., Spall, S. A. and Stouffer, R.: Response of ocean ecosystems to climate warming, Global Biogeochemical Cycles, 18(3), doi:10.1029/2003GB002134, 2004.

Schmidtko, S., Stramma, L. and Visbeck, M.: Decline in global oceanic oxygen content during the past five decades, Nature, 542(7641), 335–339, doi:10.1038/nature21399, 2017.

Screen, J. A. and Simmonds, I.: The central role of diminishing sea ice in recent Arctic temperature
965 amplification, Nature, 464(7293), 1334–1337, doi:10.1038/nature09051, 2010.

Séférian, R., Gehlen, M., Bopp, L., Resplandy, L., Orr, J. C., Marti, O., Dunne, J. P., Christian, J. R., Doney, S. C., Ilyina, T., Lindsay, K., Halloran, P. R., Heinze, C., Segschneider, J., Tjiputra, J., Aumont, O. and Romanou, A.: Inconsistent strategies to spin up models in CMIP5: implications for ocean biogeochemical model performance assessment, Geoscientific Model Development, 9(5), 1827–1851, doi:10.5194/gmd-9-1827-2016,
970 2016.

Séférian, R., Nabat, P., Michou, M., Saint martin, D., Voldoire, A., Colin, J., Decharme, B., Delire, C., Berthet, S., Chevallier, M., Sénési, S., Franchistéguy, L., Vial, J., Mallet, M., Joetzjer, E., Geoffroy, O., Guérémy, J.-F.,

Moine, M.-P., M'Sadek, R., Ribes, A., Rocher, M., Roehrig, R., Salas y mélia, D., Sanchez, E., Terray, L.,
Valcke, S., Waldman, R., Aumont, O., Bopp, L., Deshayes, J., Éthé, C. and Madec, G.: Evaluation of CNRM
975   Earth System model, CNRM ESM 2 1: role of Earth system processes in present day and future climate,
Journal of Advances in Modeling Earth Systems, doi:10.1029/2019MS001791, 2019.

Séférian, R., Berthet, B., Yool, A., Palmiéri, J., Bopp, L., Tagliabue, A., Kwiatkowski, L., Christian, J., Gehlen,
M., Ilyina, T., John, J. G., Li, H., Luo, J. Y., Romanou, A., Schwinger, J., Stock, C., Takano, Y., Tjiputra, J.,
Tsujino, H., Watanabe, M., Wu, T., Wu, F., Yamamoto, A.; Tracking improvement in simulated marine
980   biogeochemistry between CMIP5 and CMIP6, Current Climate Change Reports, in review.

Sellar, A. A., Jones, C. G., Mulcahy, J., Tang, Y., Yool, A., Wiltshire, A., O'connor, F. M., Stringer, M., Hill,
R., Palmieri, J., Woodward, S., Mora, L., Kuhlbrodt, T., Rumbold, S., Kelley, D. I., Ellis, R., Johnson, C. E.,
Walton, J., Abraham, N. L., Andrews, M. B., Andrews, T., Archibald, A. T., Berthou, S., Burke, E., Blockley,
E., Carslaw, K., Dalvi, M., Edwards, J., Folberth, G. A., Gedney, N., Griffiths, P. T., Harper, A. B., Hendry, M.
985   A., Hewitt, A. J., Johnson, B., Jones, A., Jones, C. D., Keeble, J., Liddicoat, S., Morgenstern, O., Parker, R. J.,
Predoi, V., Robertson, E., Siahaan, A., Smith, R. S., Swaminathan, R., Woodhouse, M. T., Zeng, G. and
Zerroukat, M.: UKESM1: Description and evaluation of the UK Earth System Model, Journal of Advances in
Modeling Earth Systems, doi:10.1029/2019MS001739 .

Serreze, M. C., Barrett, A. P., Slater, A. G., Steele, M., Zhang, J. and Trenberth, K. E.: The large-scale energy
990   budget of the Arctic, Journal of Geophysical Research: Atmospheres, 112(D11), doi:10.1029/2006JD008230,
2007.

Smale, D. A., Wernberg, T., Oliver, E. C. J., Thomsen, M., Harvey, B. P., Straub, S. C., Burrows, M. T.,
Alexander, L. V., Benthuysen, J. A., Donat, M. G., Feng, M., Hobday, A. J., Holbrook, N. J., Perkins-
Kirkpatrick, S. E., Scannell, H. A., Gupta, A. S., Payne, B. L. and Moore, P. J.: Marine heatwaves threaten
995   global biodiversity and the provision of ecosystem services, Nature Climate Change, 1, doi:10.1038/s41558-019-
0412-1, 2019.

Sorte, C. J. B., Williams, S. L. and Carlton, J. T.: Marine range shifts and species introductions: comparative
spread rates and community impacts, Global Ecology and Biogeography, 19(3), 303–316, doi:10.1111/j.1466-
8238.2009.00519.x, 2010.

1000   Steinacher, M., Joos, F., Frölicher, T. L., Plattner, G.-K. and Doney, S. C.: Imminent ocean acidification in the
Arctic projected with the NCAR global coupled carbon cycle-climate model, Biogeosciences, 6(4), 515–533,
doi:10.3929/ethz-b-000020082, 2009.

Steinacher, M., Joos, F., Frölicher, T. L., Bopp, L., Cadule, P., Cocco, V., Doney, S. C., Gehlen, M., Lindsay,
K., Moore, J. K., Schneider, B. and Segschneider, J.: Projected 21st century decrease in marine productivity: a
1005   multi-model analysis, Biogeosciences, 7(3), 979–1005, doi:10.5194/bg-7-979-2010, 2010.

Steiner, N. S., Christian, J. R., Six, K. D., Yamamoto, A. and Yamamoto Kawai, M.: Future ocean acidification
in the Canada Basin and surrounding Arctic Ocean from CMIP5 earth system models, Journal of Geophysical
Research: Oceans, 119(1), 332–347, doi:10.1002/2013JC009069, 2014.

Stock, C. A., Dunne, J. P. and John, J. G.: Drivers of trophic amplification of ocean productivity trends in a
1010   changing climate, Biogeosciences, 11(24), 7125–7135, doi:10.5194/bg-11-7125-2014, 2014.

Stock, C. A., Dunne, J. P., Fan, S., Ginoux, P., John, J. G., Krasting, J. P., Laufkötter, C., Paulot, F. and Zadeh, N.,: Ocean Biogeochemistry in GFDL's Earth System Model 4.1 and its Response to Increasing atmospheric CO2, Journal of Advances in Modeling Earth Systems. 2019MS002043, in review.

1015   Stramma, L., Johnson, G. C., Sprintall, J. and Mohrholz, V.: Expanding Oxygen-Minimum Zones in the Tropical Oceans, Science, 320(5876), 655–658, doi:10.1126/science.1153847, 2008.

Stramma, L., Oschlies, A. and Schmidtko, S.: Mismatch between observed and modeled trends in dissolved upper-ocean oxygen over the last 50 yr, Biogeosciences (BG), 9, 4045–4057, doi:Stramma, Lothar <https://orcid.org/0000-0003-1391-4808>, Oschlies, Andreas <https://orcid.org/0000-0002-8295-4013> and Schmidtko, Sunke <https://orcid.org/0000-0003-3272-7055> (2012) Mismatch between observed and modeled
1020   trends in dissolved upper-ocean oxygen over the last 50 yr.   Open Access Biogeosciences (BG), 9 (10). pp. 4045-4057. DOI 10.5194/bg-9-4045-2012 <http://dx.doi.org/10.5194/bg-9-4045-2012>., 2012.

Sunagawa, S., Coelho, L. P., Chaffron, S., Kultima, J. R., Labadie, K., Salazar, G., Djahanschiri, B., Zeller, G., Mende, D. R., Alberti, A., Cornejo-Castillo, F. M., Costea, P. I., Cruaud, C., d'Ovidio, F., Engelen, S., Ferrera, I., Gasol, J. M., Guidi, L., Hildebrand, F., Kokoszka, F., Lepoivre, C., Lima-Mendez, G., Poulain, J., Poulos, B.
1025   T., Royo-Llonch, M., Sarmento, H., Vieira-Silva, S., Dimier, C., Picheral, M., Searson, S., Kandels-Lewis, S., Coordinators, T. O., Bowler, C., Vargas, C. de, Gorsky, G., Grimsley, N., Hingamp, P., Iudicone, D., Jaillon, O., Not, F., Ogata, H., Pesant, S., Speich, S., Stemmann, L., Sullivan, M. B., Weissenbach, J., Wincker, P., Karsenti, E., Raes, J., Acinas, S. G. and Bork, P.: Structure and function of the global ocean microbiome, Science, 348(6237), doi:10.1126/science.1261359, 2015.

1030   Swart, N. C. and Fyfe, J. C.: Observed and simulated changes in the Southern Hemisphere surface westerly wind-stress, Geophysical Research Letters, 39(16), doi:10.1029/2012GL052810, 2012.

Swart, N. C., Cole, J. N. S., Kharin, V. V., Lazare, M., Scinocca, J. F., Gillett, N. P., Anstey, J., Arora, V., Christian, J. R., Hanna, S., Jiao, Y., Lee, W. G., Majaess, F., Saenko, O. A., Seiler, C., Seinen, C., Shao, A., Sigmond, M., Solheim, L., Salzen, K. von, Yang, D. and Winter, B.: The Canadian Earth System Model version
1035   5 (CanESM5.0.3), Geoscientific Model Development, 12(11), 4823–4873, doi:https://doi.org/10.5194/gmd-12-4823-2019, 2019.

Sweetman, A. K., Thurber, A. R., Smith, C. R., Levin, L. A., Mora, C., Wei, C.-L., Gooday, A. J., Jones, D. O. B., Rex, M., Yasuhara, M., Ingels, J., Ruhl, H. A., Frieder, C. A., Danovaro, R., Würzberg, L., Baco, A., Grupe, B. M., Pasulka, A., Meyer, K. S., Dunlop, K. M., Henry, L.-A. and Roberts, J. M.: Major impacts of climate
1040   change on deep-sea benthic ecosystems, Elementa: Science of the Anthropocene, 5, Art. No. 4, 2017.

Taucher, J. and Oschlies, A.: Can we predict the direction of marine primary production change under global warming?, Geophys. Res. Lett., 38(2), L02603, doi:10.1029/2010GL045934, 2011.

Taylor, K. E., Stouffer, R. J. and Meehl, G. A.: An Overview of CMIP5 and the Experiment Design, Bull. Amer. Meteor. Soc., 93(4), 485–498, doi:10.1175/BAMS-D-11-00094.1, 2011.

1045   Thomas, M. K., Kremer, C. T., Klausmeier, C. A. and Litchman, E.: A Global Pattern of Thermal Adaptation in Marine Phytoplankton, Science, 338(6110), 1085–1088, doi:10.1126/science.1224836, 2012.

Tittensor, D. P., Baco, A. R., Hall-Spencer, J. M., Orr, J. C. and Rogers, A. D.: Seamounts as refugia from ocean acidification for cold-water stony corals, Marine Ecology, 31, 212–225, doi:10.1111/j.1439-0485.2010.00393.x, 2010.

1050   Tjiputra, J. F., Goris, N., Lauvset, S. K., Heinze, C., Olsen, A.,Schwinger, J., and Steinfeldt, R.: Mechanisms and Early Detections of Multidecadal Oxygen Changes in the Interior Subpolar North Atlantic, Geophys. Res. Lett., 45, 4218–4229, https://doi.org/10.1029/2018GL077096, 2018.

Tjiputra, J. F., Schwinger, J., Bentsen, M., Morée, A. L., Gao, S., Bethke, I., Heinze, C., Goris, N., Gupta, A., He, Y., Olivié, D., Seland, Ø., and Schulz, M.: Ocean biogeochemistry in the Norwegian Earth System Model
1055   version 2 (NorESM2), Geosci. Model Dev. Discuss., https://doi.org/10.5194/gmd-2019-347, in review, 2020.

Vaquer-Sunyer, R. and Duarte, C. M.: Thresholds of hypoxia for marine biodiversity, PNAS, 105(40), 15452–15457, doi:10.1073/pnas.0803833105, 2008.

Vial, J., Dufresne, J.-L. and Bony, S.: On the interpretation of inter-model spread in CMIP5 climate sensitivity estimates, Clim Dyn, 41(11), 3339–3362, doi:10.1007/s00382-013-1725-9, 2013.

1060   Vichi, M., Manzini, E., Fogli, P. G., Alessandri, A., Patara, L., Scoccimarro, E., Masina, S. and Navarra, A.: Global and regional ocean carbon uptake and climate change: sensitivity to a substantial mitigation scenario, Clim Dyn, 37(9–10), 1929–1947, doi:10.1007/s00382-011-1079-0, 2011.

Watanabe, M. and Kawamiya, M.: Remote effects of mixed layer development on ocean acidification in the subsurface layers of the North Pacific, J. Oceanogr., 73(6), 771–784, doi:10.1007/s10872-017-0431-3, 2017.

1065   Watson, S.-A., Lefevre, S., McCormick, M. I., Domenici, P., Nilsson, G. E. and Munday, P. L.: Marine mollusc predator-escape behaviour altered by near-future carbon dioxide levels, Proceedings of the Royal Society of London B: Biological Sciences, 281(1774), 20132377, doi:10.1098/rspb.2013.2377, 2014.

Watson, S.-A., Fields, J. B. and Munday, P. L.: Ocean acidification alters predator behaviour and reduces predation rate, Biology Letters, 13(2), 20160797, doi:10.1098/rsbl.2016.0797, 2017.

1070   Yamamoto, A., Kawamiya, M., Ishida, A., Yamanaka, Y. and Watanabe, S.: Impact of rapid sea-ice reduction in the Arctic Ocean on the rate of ocean acidification, Biogeosciences, 9(6), 2365–2375, doi:https://doi.org/10.5194/bg-9-2365-2012, 2012.

Yamamoto-Kawai, M., McLaughlin, F. A., Carmack, E. C., Nishino, S. and Shimada, K.: Aragonite Undersaturation in the Arctic Ocean: Effects of Ocean Acidification and Sea Ice Melt, Science, 326(5956),
1075   1098–1100, doi:10.1126/science.1174190, 2009.

Yukimoto, S., Kawai, H., Koshiro, T., Oshima, N., Yoshida, K., Urakawa, S., Tsujino, H., Deushi, M., Tanaka, T., Hosaka, M., Yabu, S., Yoshimura, H., Shindo, E., Mizuta, R., Obata, A., Adachi, Y., and Ishii, M.: The Meteorological Research Institute Earth System Model version 2.0, MRI-ESM2.0: Description and basic evaluation of the physical component. J. Meteor. Soc. Japan, 97, 931–965, doi:10.2151/jmsj.2019-051, 2019.

1080   Ziehn, T., Chamberlain, M., Law, R., Lenton, A., Bodman, R., Dix, M., Stevens, L., Wang, Y.-P., Srbinovsky, J.: The Australian Earth System Model:ACCESS-ESM1.5, Journal of Southern Hemisphere Earth Systems Science (JSHESS), in review, 2019.

1085 **Table 1. The CMIP6 Earth system models used in this study, their individual components used to represent ocean, sea ice, and marine biogeochemistry, and the ocean impact drivers and simulations that were assessed.**

Model/reference	Ocean-sea ice	MBG	Drivers	Simulations
ACCESS-ESM1.5 (Ziehn et al., in review)	MOM5, CICE4	WOMBAT	T, pH, O_2, NO_3^-	Historical, SSP1-2.6, SSP2-4.5, SSP3-7.0, SSP5-8.5
CanESM5 (Swart et al., 2019)	NEMO 3.4.1-LIM2	CMOC	T, pH, O_2, NO_3^-	Historical, SSP1-2.6, SSP2-4.5, SSP3-7.0, SSP5-8.5
CESM2	POP2-CICE5	MARBL-BEC	T, pH, NO_3^-	Historical, SSP1-2.6, SSP2-4.5, SSP3-7.0, SSP5-8.5
CESM2-WACCM	POP2-CICE5	MARBL-BEC	T, pH, NO_3^-	Historical, SSP1-2.6, SSP2-4.5, SSP3-7.0, SSP5-8.5
CNRM-ESM2-1 (Séférian et al., 2019)	NEMOv3.6-GELATOv6	PISCESv2-gas	T, pH, O_2, NO_3^-	Historical, SSP1-2.6, SSP2-4.5, SSP3-7.0, SSP5-8.5
GFDL-CM4 (Held et al., 2019; Dunne et al., in review)	MOM6, SIS2	BLINGv2	T, pH, O_2, NO_3^-	Historical, SSP2-4.5, SSP5-8.5
GFDL-ESM4 (Dunne et al., in review; Stock et al., in review)	MOM6, SIS2	COBALTv2	T, pH, O_2, NO_3^-	Historical, SSP1-2.6, SSP2-4.5, SSP3-7.0, SSP5-8.5
IPSL-CM6A-LR (Boucher et al., in review)	NEMOv3.6-LIM3	PISCESv2	T, pH, O_2, NO_3^-	Historical, SSP1-2.6, SSP2-4.5, SSP3-7.0, SSP5-8.5
MIROC-ES2L (Hajima et al., in review)	COCO	OECO2	T, pH, O_2, NO_3^-	Historical, SSP1-2.6, SSP2-4.5, SSP3-7.0, SSP5-8.5
MPI-ESM1.2-HR (Müller et al., 2018; Mauritsen et al., 2019)	MPIOM	HAMOCC6	T, pH, O_2, NO_3^-	Historical, SSP1-2.6, SSP2-4.5, SSP3-7.0, SSP5-8.5
MRI-ESM2 (Yukimoto et al., 2019)	MRICOM4	NPZD	T, pH, O_2, NO_3^-	Historical, SSP5-8.5
NorESM2-LM (Tjiputra et al., in review)	BLOM- CICE5	iHAMOCC	T, pH, O_2, NO_3^-	Historical, SSP1-2.6, SSP2-4.5, SSP3-7.0, SSP5-8.5
UKESM1-0-LL (Sellar et al., 2019)	NEMO v3.6, CICE	MEDUSA-2	T, pH, O_2, NO_3^-	Historical, SSP1-2.6, SSP2-4.5, SSP3-7.0, SSP5-8.5

1090

1095

1100

1105 **Table 2. The CMIP5 Earth system models used in this study, their individual components used to represent ocean, sea ice, and marine biogeochemistry, and the simulations that were assessed.** All models provided temperature, pH, oxygen and nitrate outputs.

Model/reference	Ocean-sea ice	MBG	Simulations
CESM1-BGC (Gent et al., 2011)	POP2-CICE4	BEC	Historical, RCP4.5, RCP8.5
CMCC-ESM (Vichi et al., 2011; (Cagnazzo et al., 2013)	OPA8-2-LIM2	PELAGOS	Historical, RCP8.5
GFDL-ESM2G (Dunne et al., 2012)	GOLD	TOPAZ2	Historical, RCP2.6, RCP4.5, RCP6.0, RCP8.5
GFDL-ESM2M (Dunne et al., 2012)	MOM5	TOPAZ2	Historical, RCP2.6, RCP4.5, RCP6.0, RCP8.5
HadGEM2-ES (Collins et al., 2011)	UM	Diat-HadOCC	Historical, RCP2.6, RCP4.5, RCP6.0, RCP8.5
IPSL-CM5A-LR (Dufresne et al., 2013)	NEMOv3.2-LIM2	PISCES	Historical, RCP2.6, RCP4.5, RCP6.0, RCP8.5
IPSL-CM5A-MR (Dufresne et al., 2013)	NEMOv3.2-LIM2	PISCES	Historical, RCP2.6, RCP4.5, RCP8.5
MPI-ESM-LR (Giorgetta et al., 2013)	MPIOM	HAMOCC5-2	Historical, RCP2.6, RCP4.5, RCP8.5
MPI-ESM-MR (Giorgetta et al., 2013)	MPIOM	HAMOCC5	Historical, RCP2.6, RCP4.5, RCP8.5
NorESM1-ME (Bentsen et al., 2013)	MICOM-CICE4	HAMOCC5.1	Historical, RCP2.6, RCP4.5, RCP6.0, RCP8.5

1110

1115

1120

1125

Table 3. Global mean changes in multiple ocean impact drivers across the CMIP6 and CMIP5 ensembles.
Global mean anomalies of sea surface temperature, surface ocean pH, subsurface dissolved O_2 concentration
(averaged between 100-600 m) and upper-ocean NO_3^- (averaged between 0-100 m) for the CMIP6 SSPs and
CMIP5 RCPs. Anomalies are given as 2080-2099 mean values relative to the 1870-1899 mean. Uncertainty
estimates are the inter-model standard deviation.

1130

	CMIP5				CMIP6			
	RCP2.6	RCP4.5	RCP6.0	RCP8.5	SSP1-2.6	SSP2-4.5	SSP3-7.0	SSP5-8.5
ΔSST (°C)	+1.15± 0.33	+1.74± 0.44	+1.82± 0.54	+3.04± 0.62	+1.42± 0.32	+2.10± 0.43	+2.89± 0.61	+3.48± 0.78
ΔpH	-0.14 ±0.001	-0.21 ±0.002	-0.27 ±0.004	-0.38 ±0.005	-0.16 ±0.002	-0.26 ±0.003	-0.35 ±0.003	-0.44 ±0.005
ΔO_2 (mmol m^{-3})	-3.71 ±2.47	-6.16 ±2.86	-6.56 ± 3.27	-9.51 ± 2.13	-6.36 ±2.92	-8.14 ±4.08	-12.44 ± 4.40	-13.27 ± 5.28
ΔNO_3^- (mmol m^{-3})	-0.38 ±0.15	-0.51 ±0.14	-0.60 ± 0.18	-0.66 ± 0.49	-0.53 ±0.23	-0.66 ±0.32	-0.87 ± 0.43	-1.07 ± 0.45

1135

1140

1145

1150

1155

1160

1165

1170

1175

Table 4. Global mean projected changes in benthic ocean impact drivers in CMIP6. Global mean anomalies of bottom-water temperature (°C), pH and dissolved O_2 concentration for the CMIP6 SSPs. Anomalies are 2080-2099 mean values relative to the 1870-1899 baseline period. Uncertainty estimates are the inter-model standard deviation.

1180

	SSP1-2.6	SSP2-4.5	SSP3-7.0	SSP5-8.5
ΔSST (°C)	+0.13 ± 0.03	+0.17 ± 0.04	+0.20 ± 0.04	+0.23 ± 0.04
ΔpH	-0.017 ± 0.002	-0.022 ± 0.001	-0.025 ± 0.002	-0.029 ± 0.002
ΔO_2 (mmol m^{-3})	-5.34 ± 1.99	-5.05± 2.40	-5.99 ± 2.13	-5.19 ± 2.49

1185

1190
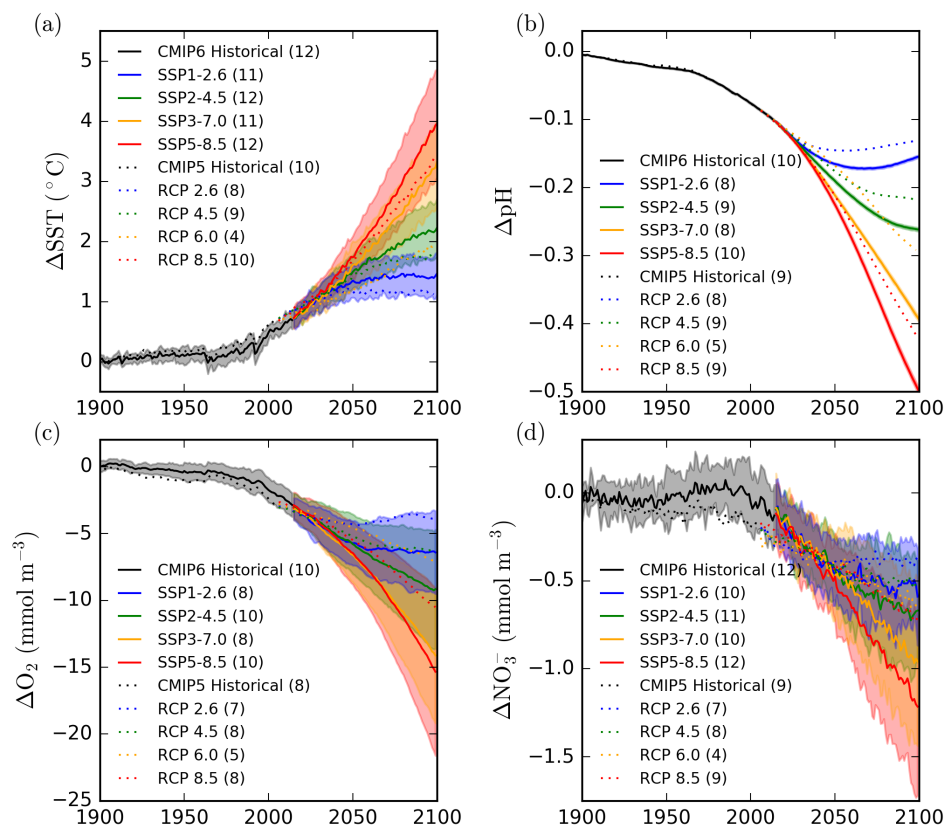
Figure 1: Global mean projections of upper-ocean impact drivers. Global mean projections of (a) sea surface temperature (°C), (b) surface ocean pH, (c) subsurface dissolved O_2 concentration (averaged between 100-600 m; mmol m^{-3}) and (d) euphotic-zone NO_3^- (averaged between 0-100 m; mmol m^{-3}). Values are anomalies relative to the 1870-1899 reference period. CMIP6 mean anomalies for the historical and SSP simulations are shown as solid lines with shading representing the inter-model standard deviation. CMIP5 projections only show the multi-model mean. The model ensemble size for each scenario is given in parentheses.
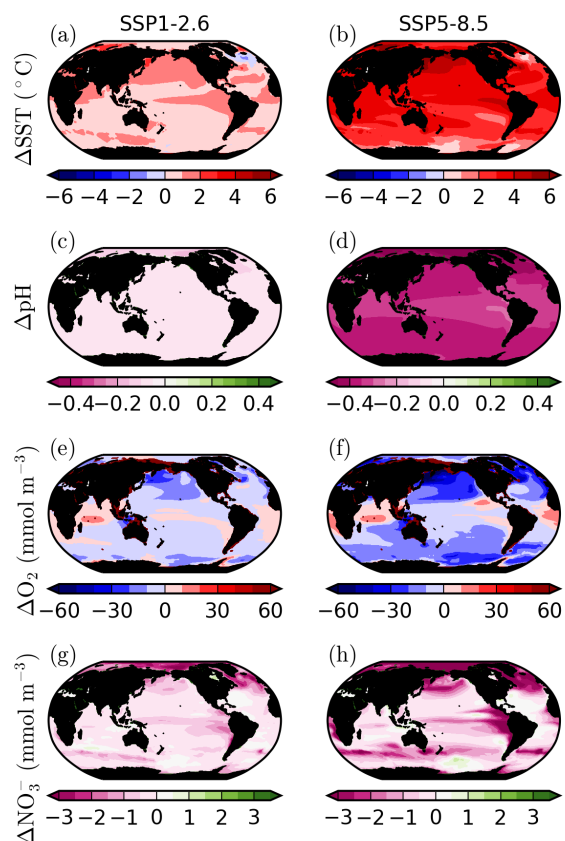
Figure 2: Projections of multiple upper-ocean impact drivers under SSP1-2.6 and SSP5-8.5. CMIP6 multi-model mean anomalies in (a-b) sea surface temperature (°C), (c-d) surface ocean pH, (e-f) subsurface dissolved O_2 concentration (averaged between 100-600 m; mmol m^{-3}) and (g-h) euphotic-zone NO_3^- (averaged between 0-100 m; mmol m^{-3}). Anomalies are 2080-2099 mean values relative to the 1995-2014 baseline period.
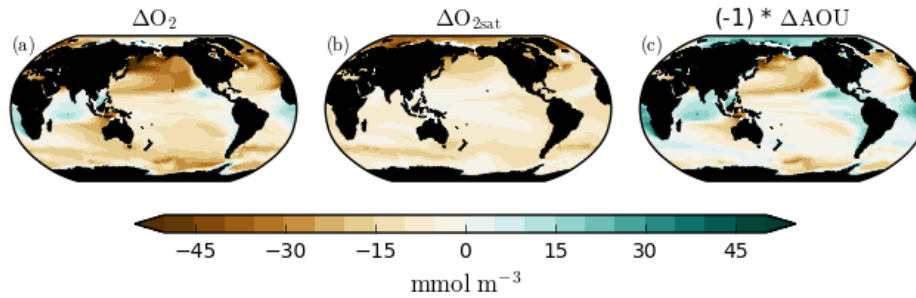
Figure 3: Change in subsurface oxygen saturation and apparent oxygen utilisation. CMIP6 multi-model mean changes in (a) subsurface dissolved O_2 concentration (averaged between 100-600 m; mmol m^{-3}), (b) subsurface O_2 saturation (O_{2sat}) and (c) subsurface apparent oxygen utilisation (AOU) in 2080–2099 of SSP5-8.5 relative to 1995–2014.

1230

1235

1240

1245

1250

1255

1260

1265
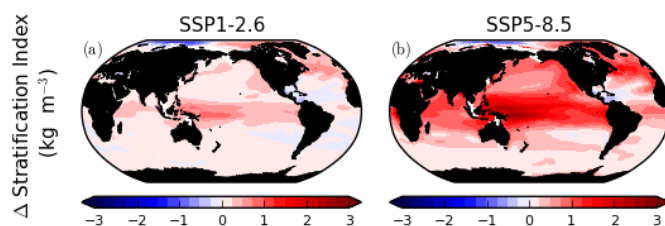
Figure 4: Change in upper ocean stratification in SSP1-2.6 and SSP5-8.5. The CMIP6 multi-model mean change in stratification index (kg m^{-3}) in (a) SSP1-2.6 and (b) SSP5-8.5. Anomalies are 2080-2099 mean values relative to 1995-2014. The stratification index is defined as the difference in density between 200 m and the surface.

1270

1275

1280

1285

1290

1295

1300
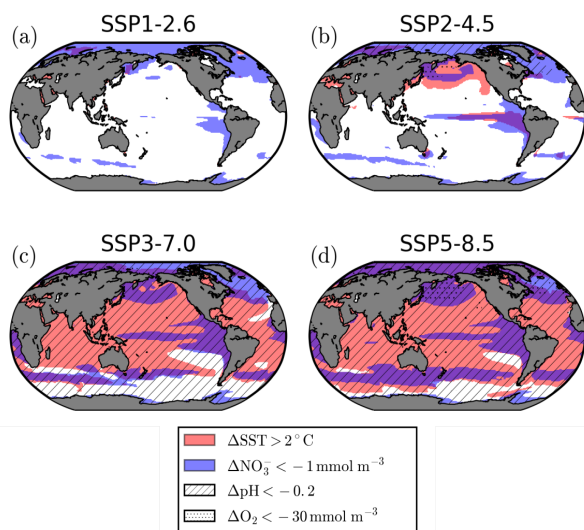
1305

Figure 5: Compound upper-ocean impact drivers. Regions where projected CMIP6 sea surface warming exceeds 2°C (red), euphotic-zone (0-100 m) NO_3^- decline exceeds 1 mmol m^{-3} (blue), surface ocean pH decline exceeds 0.2 (hatching) and subsurface (100-600 m) dissolved O_2 concentration decline exceeds 30 mmol m^{-3} (stippling) in (a) SSP1-2.6, (b) SSP2-4.5, (c) SSP3-7.0 and (d) SSP5-8.5. The exceedance of driver thresholds is

1310   determined from 2080-2099 anomalies relative to 1995-2014 values.
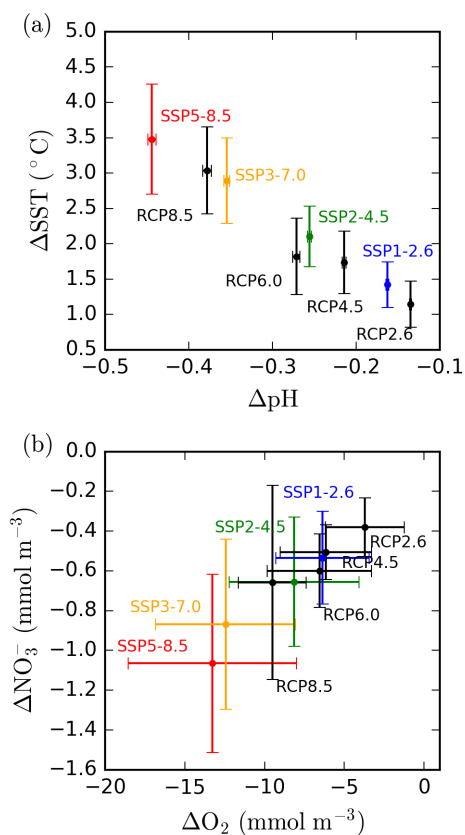
1315

Figure 6: Comparison between CMIP6 and CMIP5 end-of-century changes in upper-ocean impact drivers. Global mean anomalies of (a) sea surface temperature (°C) and surface ocean pH, and (b) subsurface dissolved O_2 concentration (averaged between 100-600 m; mmol m^{-3}) and euphotic-zone NO_3^- (averaged between 0-100 m; mmol m^{-3}) for the CMIP6 SSPs and CMIP5 RCPs. Anomalies are 2080-2099 mean values

1320 relative to the 1870-1899 baseline period. Error bars represent the inter-model standard deviation.

1325

1330
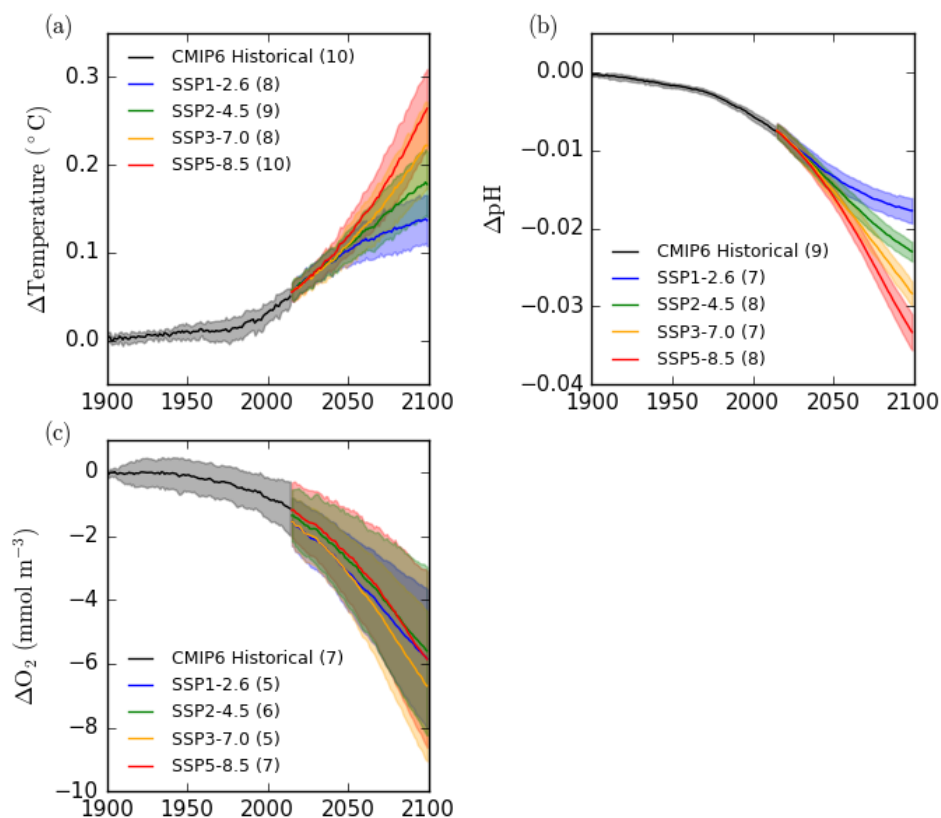
Figure 7: Global mean anomaly projections of multiple benthic ocean impact drivers. CMIP6 multi-model mean anomalies in benthic (a) temperature (°C), (b) pH and (c) dissolved O_2 concentration (mmol m^{-3}). Mean anomalies for the historical and SSP simulations are shown as solid lines with shading representing the inter-model standard deviation.. The model ensemble size for each scenario is given in parentheses.
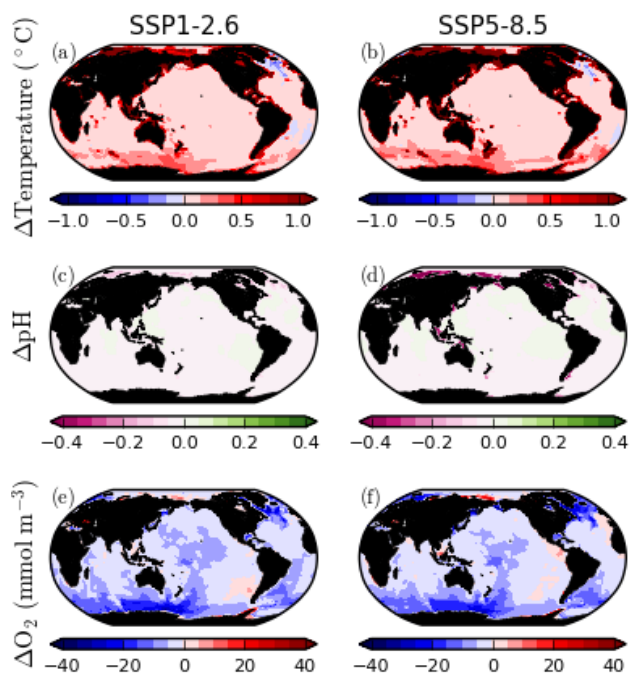
Figure 8: Projections of multiple benthic ocean impact drivers under SSP1-2.6 and SSP5-8.5. CMIP6 multi-model mean anomalies in benthic (a-b) temperature (°C), (c-d) pH and (e-f) dissolved O_2 concentration (mmol m^{-3}). Anomalies are 2080-2099 mean values relative to 1995-2014.
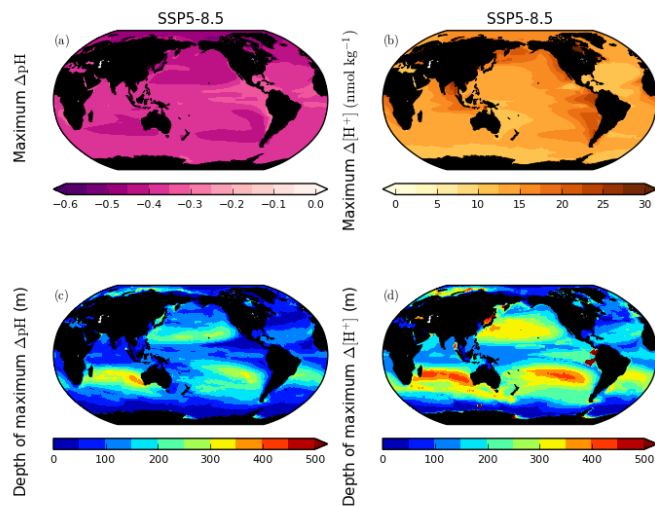
1365

1370

1375

1380

1385

1390

Figure 9: Magnitude and depth of maximum pH and [H⁺] change under SSP5-8.5. The CMIP6 ensemble mean maximum change in (a) pH and (b) [H$^+$] in 2080-2099 of SSP5-8.5 relative to 1995-2014. The mean depth at which the maximum (c) pH and (d) [H$^+$] change is projected.
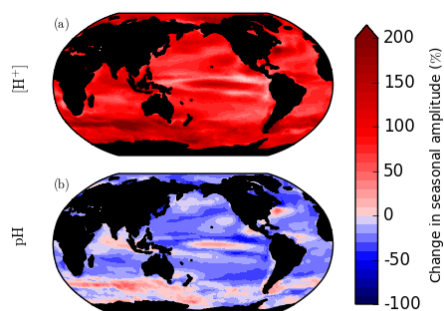
1395

1400

1405

1410

1415

1420

1425

1430

Figure 10: Change in the seasonal amplitude of surface ocean [H$^+$] and pH. The CMIP6 multi-model mean change (%) in the peak-to-peak seasonal amplitude of surface ocean (a) [H$^+$] and (b) pH under SSP5-8.5. Changes are calculated from the mean seasonal amplitude in 2080-2099 relative to that in 1995-2014.
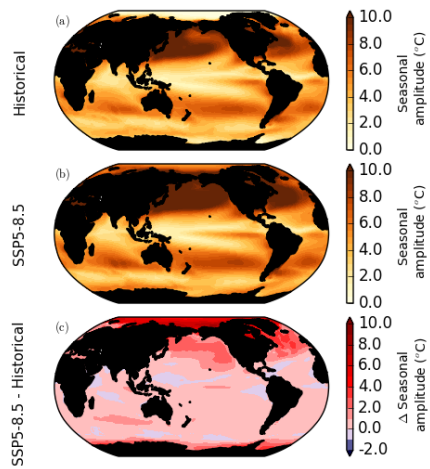
1435

1440

1445

1450

1455

1460

1465

Figure 11: The seasonal amplitude of surface ocean temperature. The CMIP6 multi-model mean peak-to-peak seasonal amplitude of surface ocean temperature (°C) in (a) 1995-2014 of the historical simulations, (b) 2080-2099 of the SSP5-8.5 simulations and (c) the change in seasonal amplitude between the two periods.

1470

1475

1480

1485